Stony Brook University

The effects of CpG and UpA dinucleotides on the attenuation of poliovirus by codon pair deoptimization

A Dissertation Presented

by

Malka Arabov

to

The Graduate School

in Partial Fulfillment of the

Requirements

for the Degree of

Doctor of Philosophy

in

Genetics

Stony Brook University

May 2014

Stony Brook University

The Graduate School

Malka Arabov

We, the dissertation committee for the above candidate for the

Doctor of Philosophy degree, hereby recommend

acceptance of this dissertation.

Eckard Wimmer – Dissertation Advisor
Distinguished Professor, Department of Molecular Genetics and Microbiology

Laurie Krug - Chairperson of Defense
Assistant Professor, Department of Molecular Genetics and Microbiology

Nancy Reich
Professor, Department of Molecular Genetics and Microbiology

Wali Karzai
Associate Professor, Department of Molecular Genetics and Microbiology

Marvin Grubman
Agricultural Research Service, U.S. Department of Agriculture

This dissertation is accepted by the Graduate School

Charles Taber
Dean of the Graduate School

Abstract of the Dissertation

The effects of CpG and UpA dinucleotides on the attenuation of poliovirus by codon pair deoptimization

by

Malka Arabov

Doctor of Philosophy

in

Genetics

Stony Brook University

2014

Codon pair bias, the preferential pairing of certain codons over others, has been observed in all species analyzed ranging from bacteria to mammals. Previous research has shown that artificial coupling of underrepresented codon pairs (codon pair deoptimization) in viral genomes (such as poliovirus and influenza virus) reduces gene function and leads to virus death or attenuation. Although the reason for this phenomenon is unclear, increasing underrepresented codon pairs in an RNA viral coding region consequently increases the frequency of CpG and UpA dinucleotides. These dinucleotides are suppressed in a variety of species and may be responsible for attenuation by codon pair deoptimization. The current study aims to determine the effects of CpG and UpA dinucleotide frequencies on viral attenuation by codon pair deoptimization.

In order to do so, four versions of poliovirus that address each characteristic (either individually or in combination with another) were designed and synthesized. Thorough analysis of these viruses indicates that increasing CpG or UpA dinucleotides, or decreasing the codon pair bias alone, affects poliovirus at different stages of infection. Specifically, while codon pair bias alone affects RNA replication or a stage upstream of replication during infection, increasing CpG dinucleotides reduces gene expression and increasing UpA dinucleotides shortens mRNA half-life. All three characteristics affect viral infectivity to varying extents. Interestingly, there does not seem to be a direct correlation between the rate of replication or protein synthesis and peak viral titer.

Although additional aspects of codon pair bias remain unclarified, the current work provides a novel route for strategic adjustment of genetic patterns during genome design depending on the objective of synthesis. These results can act as a foundation for the design of genes with altered expression, of attenuated vaccine candidates or even of gene therapy vectors with increased stability.

Dedication Page

There are a number of people who have been greatly influential in my decision to pursue a doctorate degree and who have been great supporters through the time that it took me to complete it.

I am deeply indebted to my parents, Eli and Bella, who provided the foundation on which my education has been built. They pushed me to do the best that I can at each stage of my life and displayed great pride in all of my accomplishments. My father has always taken great interest in the work that I do, and encouraged my love for the sciences and for my research. Above all else, my mother nurtured my children and me through countless days of hard work and tears (not always the babies'). She is a woman whose care for us knows no end and I cannot think of any way to repay her for that.

My sisters are my best friends. They understand the choices I make better than anyone else because we grew up with the same values. It is they, therefore, who hear me when I have problems. It is they who talk me through those problems. It is with their advice and encouragement that I have been able to reach this success. Sherry has been a role model for me for as long as I can remember, as a person, a professional, a wife, and a mother. Donna was the motivation that brought me back to the sciences and the inspiration that kept me strong through it all. I am genuinely grateful to have them both in my lives.

My husband was the biggest source of distraction from my research, in the best way possible. I married Roee halfway through the completion of my degree, and he has been the balance in my life ever since. My time outside of work developed new meaning and filled with boundless happiness, especially as he added the role of mother to my repertoire. I am grateful for the endless functional and emotional support that he has shown me through the toughest parts of writing this dissertation. As I complete the final words of this document, I know he breathes a sigh of relief along with me. My love and appreciation for him is forever growing.

My children, Aiden and Ayla, are too young to comprehend how much they have already influenced me. In watching them grow and discover their surroundings, I have witnessed the importance of learning through naïve eyes, without predispositions. It is vital to good research, but it is a skill that is difficult to master. Beyond that, my children have motivated me to better myself, professionally and personally. Each day I model the behavior that I expect of them. Each day I try to be somebody who they can look up to. As they grow older, I hope to be a continuous source of pride for them as well as an inspiration to pursue their passions. May their smiles always stay as pure as they are now.

Table of Contents

List of Figures

List of Tables

Chapter 1: Introduction

Poliovirus

Poliovirus, the causative agent of poliomyelitis, is a single stranded positive-sense nonenveloped RNA virus. It is an enterovirus belonging to the *Picornaviridea* family and its genome is approximately 7.4 kilobases in length [1]. The virus particle binds human cells via the CD155 receptor, which facilitates a conformational change in the virion [2,3]. The virus and receptor are internalized entirely and the viral RNA is uncoated shortly thereafter [4].The viral protein VPg is cleaved from the RNA to which it is bound via a cellular phosphodiesterase [5], thereby enabling translation of the genome to initiate at a 5' internal ribosome entry site (IRES) [6] (Fig 1.1).

The genome is translated as one long polypeptide, the polyprotein, which is then cleaved by virus-encoded proteinases into various structural (P1) and nonstructural (P2, P3) viral proteins [7] (Fig 1.2). The initial cleavage is the autocatalytic cleavage of $2A^{pro}$, separating P1 from P2 and P3 [8]. Further processing of P1 results in the proteins that will comprise the viral capsid (namely, VP0, VP1, VP3) [9]. Sixty copies of each of these proteins are arranged in icosahedral symmetry [10] to form the poliovirus capsid which will encapsidate a single copy of the viral RNA [11]. VP0 is cleaved into VP2 and VP4 as the virion matures and becomes infectious. The remaining proteins, which result from cleavage of P2 and P3 by viral proteases $3C^{pro}$/$3CD^{pro}$, serve as regulatory proteins essential for replication of the viral genome and for polyprotein processing. The protein complex (which is made up of 2BC, 2B, 2C, 3AB, 3A and 3B) is needed for

viral replication, while $3D^{pol}$ is the RNA-dependent RNA polymerase which is responsible for replicating the viral RNA genome[12]. Finally, the viral protein 3B (VPg) is an important primer for RNA synthesis. It is covalently attached to the 5' end of the viral RNA and becomes uridylylated by $3D^{pol}$, providing the opportunity for RNA extension [9].

During replication, the infecting positive-strand RNA acts as a template for negative strand synthesis, temporarily creating double stranded RNA structures. The negative strands will be used for production of additional positive strand RNA molecules, which in turn can be utilized as translation templates or can be packaged into the newly formed capsids and released from the cell upon lysis. The capsid protein is the determinant of cellular receptor specificity, as well as virus antigenicity, thereby categorizing poliovirus into one of three serotypes: PV1, PV2, and PV3 [13].

Although poliovirus infections most commonly remain asymptomatic after infection of the gut [13], approximately 0.1% to 1% of cases lead to infection of motor neurons of the central nervous system, causing paralytic poliomyelitis [14]. Even with a low percentage of paralysis relative to viral infection, poliomyelitis-caused epidemics left hundreds of thousands of adults and children permanently paralyzed, or even dead, around the world in the first half of the 20^{th} century.

Relief came eventually with the development of the Jonas Salk vaccine in 1952 [15] followed by the Albert Sabin vaccine in 1962 [16]. The Salk vaccine (IPV) contains inactivated polioviruses 1, 2 and 3 and is administered via injection in three doses (although some countries vaccinate in up to five doses). The production of protective

antibodies against all three serotypes efficiently immunizes 99% of its recipients. The Sabin vaccine, which is orally administered (OPV), contains a live version of the virus that replicates well in the gut, but is too attenuated to spread to the cells of the nervous system in most cases. The use of these two vaccines has greatly reduced the prevalence of polio so that it is now only endemic in Nigeria, Pakistan and Afghanistan [17].

Although poliovirus is no longer a global threat, gaps in vaccine efficiency have made eradication efforts difficult. However, a recent more aggressive push towards eradication and vaccine distribution has effectively removed India from the list of endemic countries and reduced the number of worldwide cases to the lowest ever seen: 223 cases in 2012 (Fig 1.3) [17]. In May of that year, the World Health Assembly declared polio eradication a programmatic emergency for global public health. They developed a comprehensive eradication and endgame strategy, which is to last through 2018 in order to rid the world of polio permanently: The Polio Eradication & Endgame Strategic Plan 2013-2018 (Fig 1.4). A main goal of the plan includes strengthening vaccination campaigns, particularly in endemic countries, in order to stop the transmission of wild poliovirus while simultaneously controlling outbreaks of circulating vaccine-derived poliovirus (cVDPV). A case of VDPV occurs when a population is under immunized and a vaccine strain virus is excreted and spread through the community (particularly in areas of inadequate sanitation). The normally weakened virus can acquire genetic changes as it is passed from person to person, eventually reverting to a pathogenic form that can cause paralysis just like its wild type counterpart.

About 90% of cVDPVs are caused by the type 2 strain in the traditional trivalent OPV which includes polio types 1, 2 and 3.

It is clear that successful eradication demands the development of novel low-cost inactivated vaccines, preferably produced from attenuated seed viruses that have little chance of reversion. Until then, the program recommends a shift from the use of trivalent OPV to the use of a bivalent OPV (which excludes the eradicated type 2 strain) in combination with IPV in order to reduce the number of VDPV cases worldwide.

Synthesis of Poliovirus Genomes in the Absence of Natural Templates

RNA that is extracted from poliovirus is infectious upon transfection in mammalian cells in culture [18] even though it is not covalently linked to the viral protein VPg [5,19]. This holds true for cDNA clones of the RNA genome as well, albeit at very low efficiency [20,21]. Furthermore, if cDNA of the genome is inserted downstream of a phage T7 RNA promoter, the plasmid may be used to transcribe RNA that is infectious as well at vastly higher specific infectivity [22]. Finally, infectious poliovirus may even be acquired from virion RNA that is translated in a cell-free system by incubation with cell extracts and nucleoside triphosphates [23].

With these vital tools at hand, in 2002 Eckard Wimmer and colleagues went on to publish the cell-free synthesis of poliovirus in the absence of a natural template [24]. This was done by assembling overlapping oligonucleotides into a cDNA plasmid containing a phage T7 polymerase promoter and using T7 RNA polymerase to transcribe the sequence into an infectious poliovirus RNA genome. The synthetic version of poliovirus was engineered with various synonymous mutations that were used as genetic markers ("water marks") to rule out the possibility of contamination with wild type when growing the virus in vitro.

The ability to create viable viruses by chemical synthesis based solely on sequence design of the whole genome or segments thereof has since given the Wimmer group the ability to rapidly modify large segments of the viral genome with synonymous codons without altering its amino acid sequence, leading to studies that can extend our understanding and prevention of viral disease.

Advantages of genetic recoding

Due to the redundancy of the genetic code, most amino acids can be encoded with several different codons. For example, proline can be encoded by CCT, CCC, CCA or CCG. This redundancy allows a protein to be encoded in an incredible number of ways, all of which are theoretically feasible but most of which are never found in nature. However, the ability to chemically synthesize poliovirus has paved the way for recoding the genome with various goals at hand.

Recoding has given us the opportunity to search the poliovirus genome for signals that are critical for the survival of the virus. Song et al [25] used a method called "signal location search" in which the amino acid sequence remained unchanged but the primary sequence of the poliovirus genome was altered such that it does not affect the growth of the virus unless it destroys the sequence/structure of a functional RNA element. Using this technique, in combination with classic molecular genetics, the group was able to find two functionally redundant elements in the poliovirus genome that were previously unknown. The signals, named α and β, yield wild type-like viruses if recoded individually but if both regions are altered, the virus is attenuated due to decreased viral replication.

In addition, the ability to chemically synthesize redesigned sequences has made it possible to further our understanding of the redundancy of the genetic code. Specifically, it has been shown that some codons are used more frequently to encode an amino acid than others, a phenomenon known as codon bias. For example, in

human genes, the leucine codon CTG is used 40% of the time, whereas the synonymous codon CTA is only used 7% of the time. The bias varies in different species and evidence suggests that it is correlated with the number of tRNA copies there are in the genome that recognize given codons [26]. Codon bias has been extensively studied but the evolutionary significance of it is still largely unclear.

In 2006 Mueller et al recoded the capsid region of poliovirus such that many of the wild type codons were replaced by synonymous codons that are underrepresented in the human genome (since humans are the natural host for poliovirus) [27]. This codon bias deoptimized virus, named PV-AB, was compared to a second synthetic virus, PV-SD, in which synonymous codons were randomly shuffled within the region and which served as an internal control. In both cases, the P1 capsid region was chosen for computer-aided recoding and synthesis because there is no evidence of replication signals in that region that would affect viral growth [28]. PV-SD behaved similarly to wild type in growth curves and created plaques similar in phenotype as those made by wild type. This virus provided evidence that recoding and chemically synthesizing the capsid region of poliovirus is not in itself hazardous to the virus. In contrast, PV-AB was not viable at all until portions of it were subcloned into a wild type background. The subcloned viruses still exhibited an attenuated phenotype as evidenced by decreased growth and smaller plaque sizes. Further characterization of the viruses provided evidence that decreased protein levels were at least in part responsible for the viral attenuation [27].

Codon pair bias

Codon pair bias refers to the preferential pairing of certain codons over others regardless of codon bias. For instance, on the basis of codon frequencies in human genes, the amino acid pair Ala-Glu is expected to be encoded by GCC-GAA and GCA-GAG about equally often. However, in reality, the codon pair GCC-GAA is strongly under-represented despite the fact that it contains the most frequently used Ala codon. Although codon pair bias differs between species such as bacteria, yeast, and mammals, closely related mammals exhibit nearly identical codon pairing trends. The reasons behind this phenomenon, and biological implications underlying it, have yet to be resolved, but several factors may play a role in this preferential pairing.

The over- or under-representation of each possible codon pair can be calculated as a codon pair score (CPS) by taking the natural log of the observed over expected number of occurrences of the pair over a large number of known genes in the given species. The expected values take into consideration the frequency of each codon in the pair, as well as the frequency of the encoded amino acid pairs. Under-represented pairs yield negative values, while over-represented scores yield positive values. The codon pair bias (CPB) of a gene is then calculated by taking the average of the codon pair scores over the length of the open reading frame (Fig. 1.5, [29]). Using these equations, the human codon pair bias was calculated for 14,795 annotated human genes and plotted against gene length (Fig. 1.6, [29]). The plot forms a bell-shaped curve, with most long and intermediately sized genes falling slightly above zero. Small genes showed more variability.

To study the significance of codon pair bias, the potential to synthetically recode the poliovirus genome once again became a valuable tool. Specifically designed computer software, which is capable of shuffling all the existing codons while maintaining an identical amino acid sequence, was instructed to create two new versions of poliovirus. These were to include either mostly overrepresented human codon pairs or underrepresented human codon pairs in the P1 capsid coding sequence, namely P1-Max and P1-Min, respectively [29]. Unlike P1-AB [27], the codon usage in these two viruses was identical to wild type as the existing codons in the genome were simply relocated in order to create new codon pairs (Fig 1.7). The recoding was done relative to the human host because poliovirus overcomes human cells and hijacks their cellular machinery.

In characterizing the two viruses, Coleman *et al.* found that P1-Max behaved similarly to wild type in cell culture, i.e. single step growth kinetics, translation and plaque size, while P1-Min was nonviable. Portions of the codon pair "deoptimized" region of P1-Min were subcloned into a wild type backbone and thus produced viable yet attenuated viruses. These P1-Min derivatives portrayed decreased infectivity, smaller plaques and a defect in translational efficiency in comparison with wild type. Additionally, in polio-sensitive CD155 transgenic mice [30,31], P1-Min subclones required higher doses than wild type in order to cause disease whereas P1-Max was neurovirulent at low doses like wild type when administered to mice intracerebrally.

The computer-based codon pair deoptimization approach may be extended to other pathogens as well. For example, segments of the influenza virus genome were codon pair deoptimized in a fashion similar to poliovirus in a search for flu vaccine

candidates. The recoded viruses exhibited decreased protein synthesis in cell culture but produced a robust immune response which protected against subsequent challenge with the wild type influenza virus in animal models [32,33]. Experiments with the codon pair deoptimized *ply* gene of *Streptococcus pneumonia* revealed comparable results, namely decreased production of pneumolysin in cell culture and reduced virulence in mice with a robust immune response [34].

Given the plasticity of this method, it can be applied to a variety of genes in different pathogens with hopes of quickly creating attenuated viruses as vaccine candidates, with little likelihood of reversion (due to the hundreds of changes in the genome). Therefore, experiments with Vesicular Stomatitis virus and Dengue virus are currently underway in our laboratory as well. These are of particular interest due to their ability to live in two vastly different species, insects and mammals, with diverse codon pair biases. Therefore, their genes can be deoptimized with respect to the codon pair bias of one or both species depending on the goal at hand.

Dinucleotide Content

Although reducing the codon pair score of a gene does not affect codon bias, it introduces a high number of CpG and UpA dinucleotides into the gene, because many of the underrepresented human codon pairs include these dinucleotides at the N_3-N_1 ($N_1N_2\mathbf{N_3}$-$\mathbf{N_1}N_2N_3$) position of the codon pair as depicted in figure 1.8. In all codon positions, UpA and CpG dinucleotides have been found to be strongly suppressed in the genomes of many organisms. The suppression was characterized originally in plant and animal cells [35,36] then extended to include a large variety of categories of life [37,38].

UpA dinucleotide suppression has been shown in coding DNA universally. For example, all eukaryotic and prokaryotic genomes are UpA suppressed, as well as the RNA viruses [39,40], and DNA viruses (including retroviruses) [38] that infect them. Interestingly, nontranscribed DNA sequences such as Y chromosomal DNA and mitochondrial DNA are not UpA suppressed but DNA encoding nontranslated RNA (i.e. rRNA and tRNA) is [41]. Given that UpA dinucleotides are most stringently underrepresented in sequences destined to be expressed as mRNA in the cytoplasm, it has been suggested that these dinucleotides act as substrates for cleavage by endoribonucleases [41]. Studies done *in vitro* with cell extracts and *in vivo* showing increased degradation of mRNA containing elevated UpA content [42,43] provide evidence of preferential cleavage.

In contrast, scarcity of CpGs is thought to be a result of DNA methylation, since it is seen primarily in vertebrates and many vertebrate viruses [39,40], but not at all in

nonvertebrate eukaryotes or in prokaryotes. Between 60-90% of vertebrate CpGs are methylated and are susceptible to spontaneous deamination of 5-methylcytosine to thymine, yielding an increase of TpG dinucleotides [44-46], whereas nonvertebrate genomes are less commonly methylated. Furthermore, unmethylated CpG dinucleotides, such as those found in bacterial DNA, have been shown to stimulate the innate immune system by interaction with TLR9 resulting in the production of proinflammatory cytokines such as interferon [47,48], an observation suggesting that recognition of CpG motifs is an important part of a rapid response to microbial infection [49]. It has also been shown that single stranded RNA oligoribonucleotides containing unmethylated CpG motifs can also stimulate an immune response by acting directly on monocytes [50]. Such efficient recognition and rapid response by the host may have been the influential factors for vertebrate viruses to evolve CpG suppression as well.

The synthetic virus P1-Min [29] had a low codon pair score and a relatively high number of CpG and UpA dinucleotides. Coleman et al. [29], however, did not differentiate whether the nonviability of this recoded virus was in fact due to codon pair deoptimization or if the artificial increase of the normally suppressed dinucleotides was the prevailing determinant. The authors merely concluded that slowed or defective protein synthesis was the cause for attenuation of subclones of PV-Min.

A study released shortly thereafter by Burns *et al* [51] showed that increasing CpG and UpA dinucleotides in poliovirus genomes decreases the virus' infectivity. The group systematically changed existing codons in the capsid region to increase these dinucleotides in different positions of the codons: within codons (N_1-N_2, N_2-N_3) and/or across codons (N_3-N_1). As a result, their constructs had altered codon bias, codon pair

bias, or both. One of their constructs (ABc_{12}) had a normal codon pair score and high CpG and UpA content. The decreased infectivity in ABc_{12} led the group to conclude that the attenuation seen in the previously published subclones of PV-Min [29] was not related to codon pair bias but rather to the increased CpG and UpA content. However, ABc_{12} also decreased the codon bias of the genome, whereas the codon bias of PV-Min was unchanged. It is possible that ABc_{12} was attenuated due to decreased codon bias, a phenomenon that has been previously observed [27,52]. More recently, Atkinson et al. [53] showed that increasing CpG and UpA dinucleotides caused attenuation of echovirus 7 by decreasing growth, specific infectivity and plaque size.

The experiments by Burns [51] and Atkinson [53] did not adequately address the roles of codon pair bias and dinucleotide frequency in viral attenuation. Therefore, the purpose of the current study is to determine which feature (codon pair bias or dinucleotide frequencies) plays a pivotal role in viral attenuation and ultimately to elucidate the mechanism by which codon pair bias affects viral growth.

Chapter 1 Figures

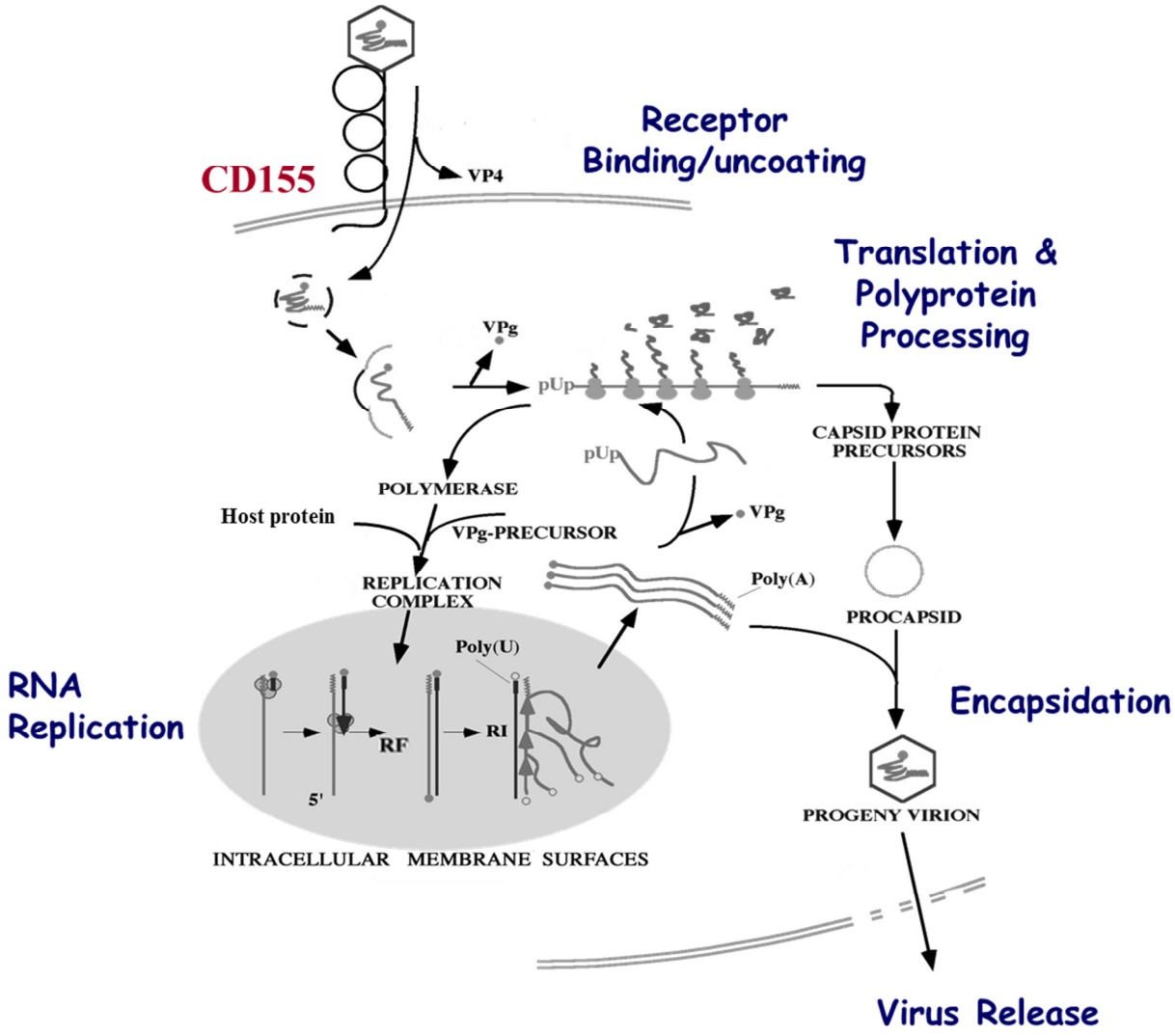

Figure 1.1: Poliovirus life cycle. Poliovirus binds its receptor (CD155), is internalized, and the viral RNA is uncoated. VPg is cleaved by cellular phosphodiesterases and IRES mediated translation is initiated. The polyprotein is processed, yielding structural and nonstructural proteins. Positive sense RNA serves as a template for negative strand synthesis. The negative sense RNA can initiate synthesis of many positive sense RNAs which in turn serve as more templates or become encapsidated by viral proteins. Progeny virions are released when the cell lyses. Adapted from [54].

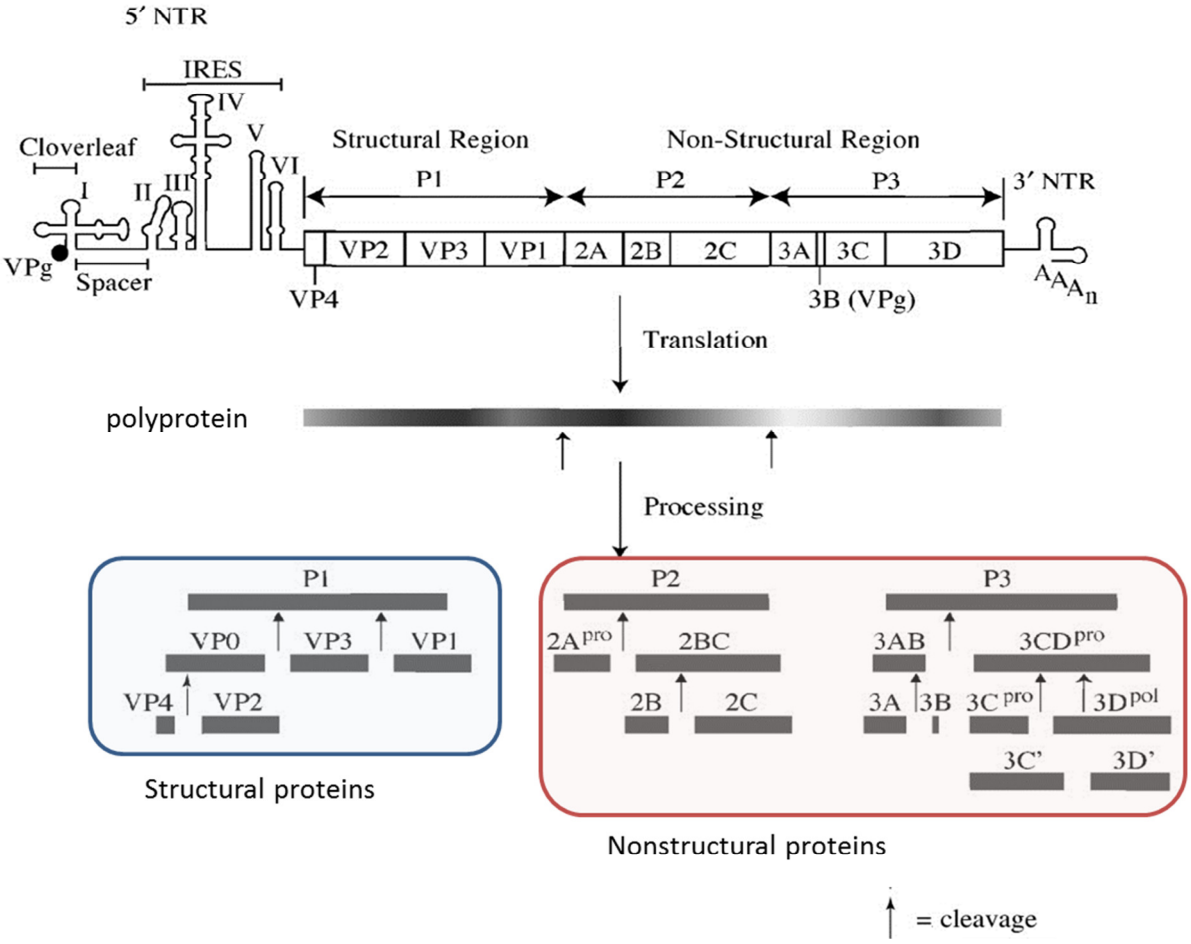

Figure 1.2: Poliovirus genome and polyprotein processing. The poliovirus genome is 7.4kb and is RNA of plus stranded polarity. At the 5' end it is covalently linked to the small viral protein VPg followed by a long nontranslated region, including an internal ribosome entry site. The open reading frame encodes a long polyprotein which is then cleaved into functional proteins. P1 is the precursor to the capsid proteins, whereas P2 and P3 are cleaved into replication proteins. The ORF is followed by a 3' nontranslated region. Adapted from [7].

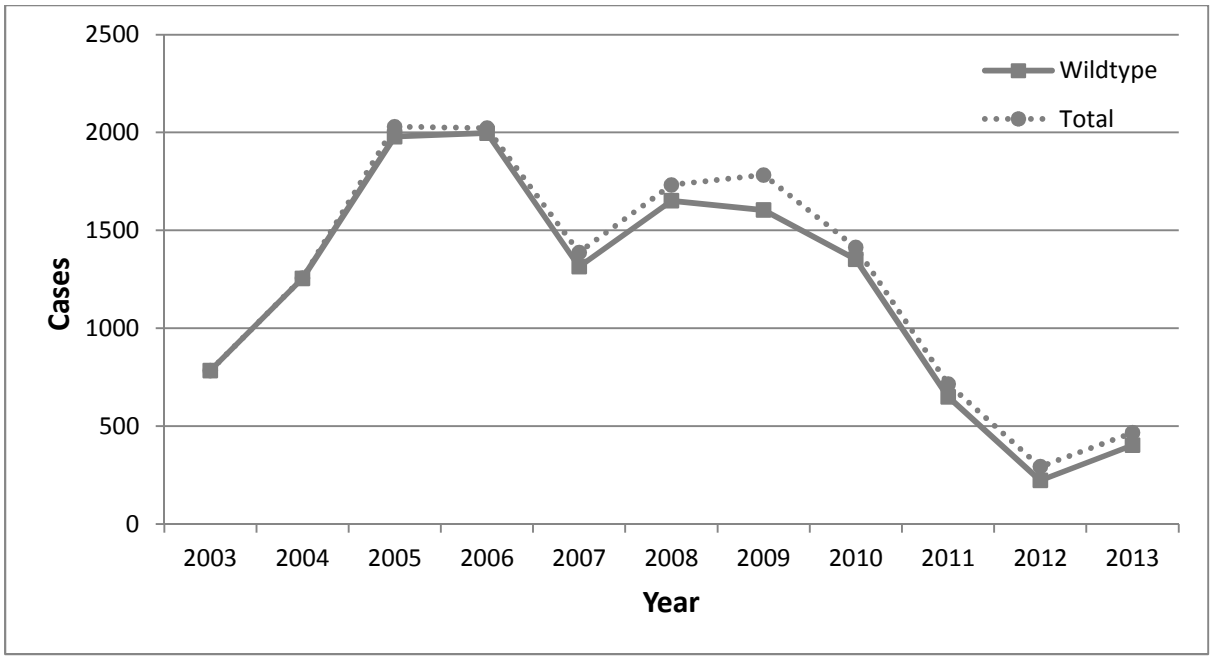

Figure 1.3: Incidence of confirmed poliomyelitis worldwide over the last decade. Confirmed wild type cases are plotted with a solid line while total confirmed cases, which include circulating vaccine-derived poliovirus, are plotted with a dotted line. [17]

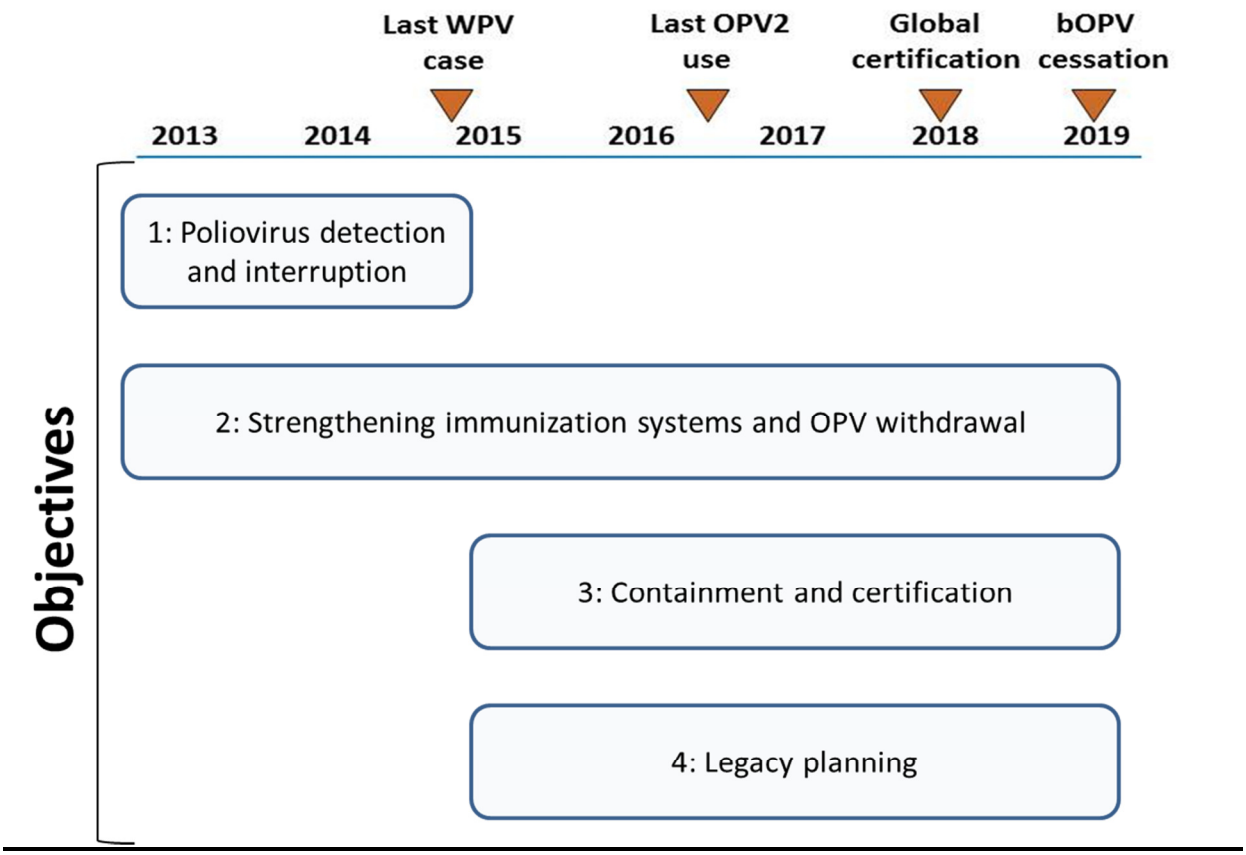

Figure 1.4: The Polio Eradication & Endgame Strategic Plan. The World Health Association developed this comprehensive poliovirus eradication and endgame strategy which is to last through 2018 in order to rid the world of polio permanently. Objectives and expected completion dates are shown. Adapted from [17].

A

$$CPS = \ln\left(\frac{F(AB)_O}{\frac{F(A) \times F(B)}{F(X) \times F(Y)} \times F(XY)}\right)$$

where AB represents a codon pair encoding the amino acid pair XY

B

$$CPB = \sum_{i=1}^{k} \frac{CPS_i}{k-1}$$

Figure 1.5: Codon pair score and codon pair bias equations. (A) The equation for the codon pair score of a specific codon pair is a function of the observed frequency of the codon pair versus the relative expected frequency, normalized for codon and amino acid usage. The codon pair AB encodes for amino acid pair XY, and F denotes frequency. Over-represented pairs in the human genome will have a positive value, whereas under-represented pairs will be negative. (B) The codon pair bias is the arithmetic mean of the individual codon pair scores of the open reading frame. [29]

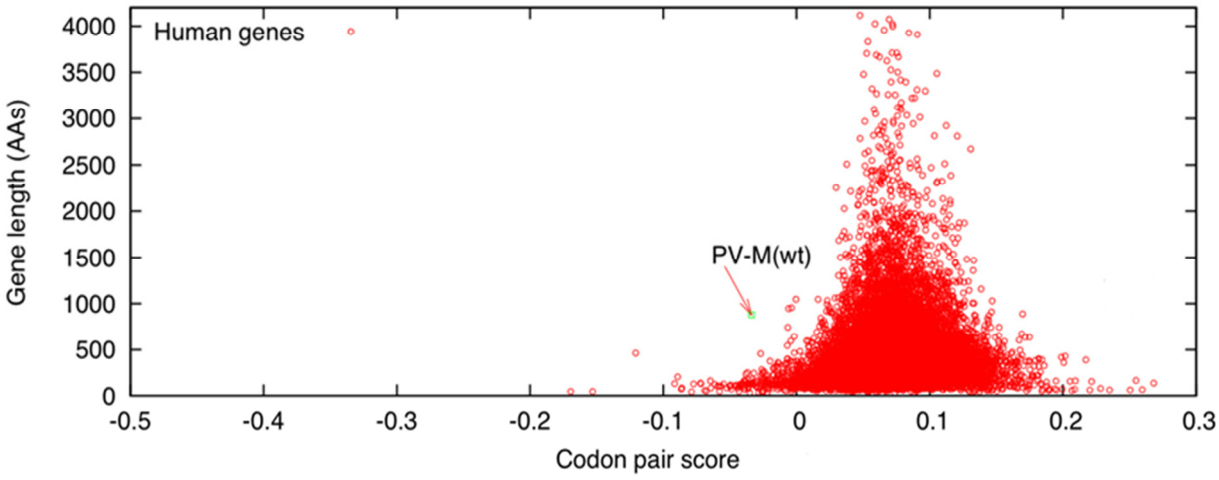

Figure 1.6: Human gene length vs codon pair bias. Codon pair biases (CPB) for 14,795 annotated human genes. Each red dot represents the CPB of a gene plotted against its amino acid length. Underrepresented codon pairs yield negative scores. CPB of wild type poliovirus (CPB = –0.02) was calculated using codon pair scores of the human genome [29]

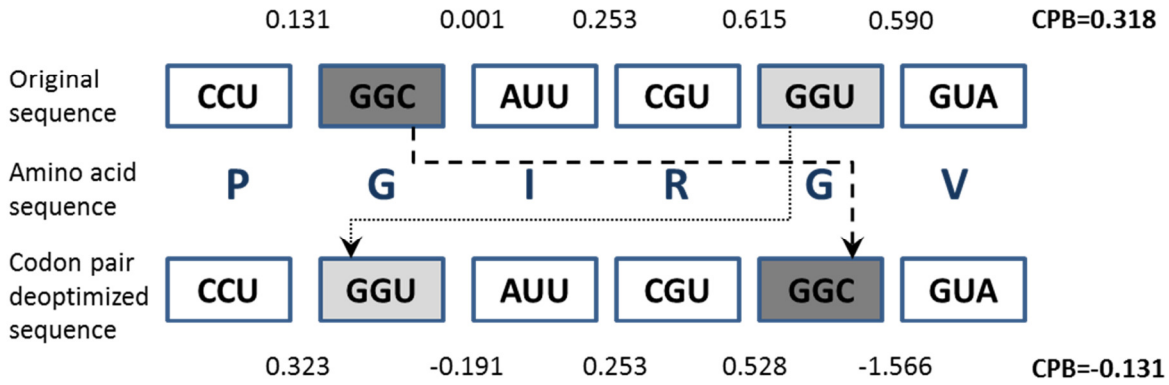

Figure 1.7: Diagram of codon shuffling. Codons in original sequence are shuffled in order to alter codon pair bias. The middle row represents the amino acid sequence that is encoded. The boxed triplets are codons that correspond to the amino acids. Above and below each codon pair is the respective codon pair score as calculated according to human genes. In bold on the right is the codon pair bias that is calculated by averaging the codon pair scores over the open reading frame. Arrows represent movement of existing codons to alter the codon pair bias. In this particular case the ORF is codon pair deoptimized as signified by a decrease in CPB.

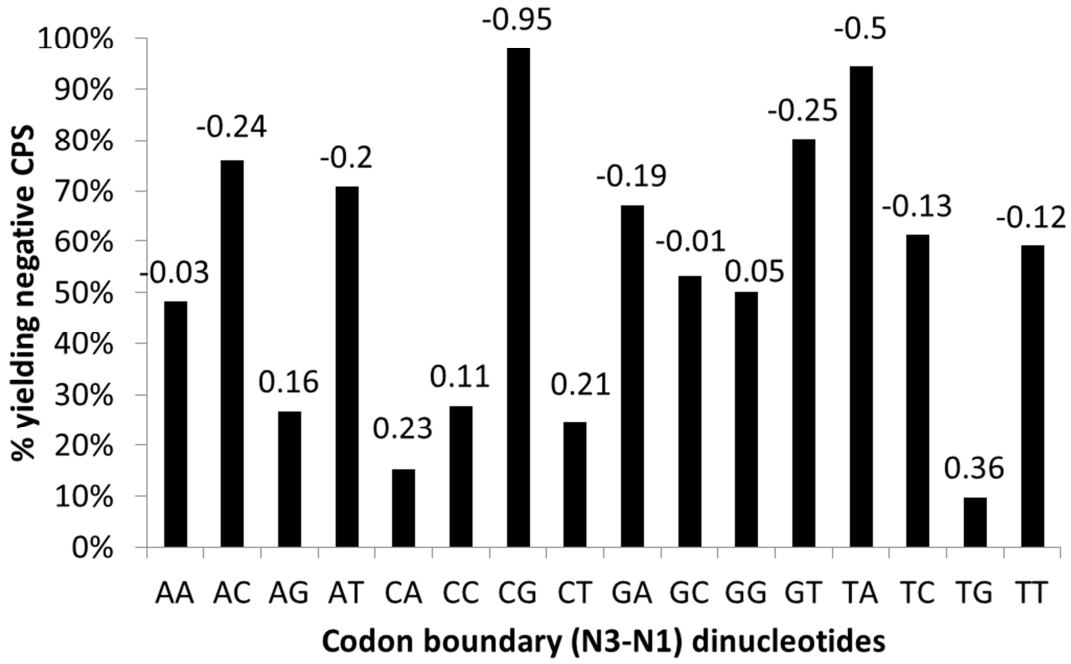

Figure 1.8: Frequency of N_3-N_1 dinucleotides in negative codon pairs. The bar graph represents the percent of codon pairs containing the designated N_3-N_1 dinucleotide that yields a negative codon pair score. The value above each bar is the average codon pair score from all the codon pairs with the designated N_3-N_1 dinucleotide. For example, of all the codon pairs XX**A**-**A**XX (AA dinucleotide), 48% of them are negative and the average CPS for these codon pairs is -0.03.

Chapter 2: Assembly of synthetic viruses and their proliferation in cell culture

Synthetic Virus Design

In order to tease apart the effects of codon pair bias and dinucleotide frequency on the phenotype of poliovirus, four new viruses were designed in which the capsid region of the viral genome was replaced with redesigned sequences, which code for the same amino acid sequence. The computer algorithm that was used to do so has been previously described [29] and is able to shuffle the existing synonymous codons in a sequence to make novel pairs to increase or decrease the codon pair bias depending on the goal. If underrepresented codon pairs (those with low codon pair scores) are selected for, the codon pair bias of the gene decreases. If overrepresented codon pairs (those with high codon pair scores) are selected, the codon pair bias of the gene increases. It can also change or maintain dinucleotide frequencies as desired by the user. Since the algorithm does not introduce new codons, codon bias is not altered.

The recoded viruses in this study vary in codon pair bias and in the frequencies of CpG or UpA dinucleotides. P1-CG^{hi} contains a codon pair bias similar to wild type but a very high CpG content. Similarly, P1-UA^{hi} contains a very high UpA content but a codon pair bias similar to wild type. P1-CPB^{lo} contains many underrepresented codon pairs (a low codon pair bias) with CpG and UpA values similar to wild type. Finally, P1-$CPB^{lo}UA^{hi}$ has a low codon pair bias as well as an excess of UpA dinucleotides as compared with wild type. In designing the viruses, codons were swapped within the

capsid in order to preserve codon use; therefore all increases of dinucleotides were in the N3-N1 positions of the codons. Codon pair biases, dinucleotide frequencies and number of silent mutations over the length of the entire genome for each of these viruses are summarized in Table 2.1, along with those for P1-Min, P1-Max, P1-AB and P1-SD as reference. Notably, P1-Min had a low codon pair score but also high concentrations of CpG and UpA dinucleotides [29].

Production and Purification of Infectious Virus

Plasmids containing portions of viral genomes were produced commercially and assembled into pT7-PVM plasmids using basic cloning techniques. Viral RNAs were produced in vitro using T7 polymerase and then transfected into HeLa cells. RNA from each of the five viruses was infectious, as evidenced by cpe within the cells. P1-WT, P1-CG^{hi}, P1-UA^{hi} and P1-CPB^{lo} displayed complete cpe by 24 hours post infection, whereas P1-CPB^{lo}UA^{hi} was delayed but displayed complete cpe by 48 hours.

Supernatants from dishes containing transfected cells were used to reinfect naïve cells in order to amplify the viruses. Amplified virus was purified on a sucrose cushion such that only encapsidated RNA remained at completion. All experiments described herein were conducted with purified virus in order to avoid the introduction of residual transcription factors, cytokines or non-encapsidated viral RNA from previous infections.

Specific Infectivities and Plaque Phenotypes

Once purification was complete, the concentration of viral particles was determined for each virus by spectrophotometric readings at OD_{260} using the formula *$1OD_{260}$ unit=$9.4x10^{12}$ particles [13]*. The results are summarized in Table 2.2. In parallel, the same virus stock was titered by plaque assay as previously described [23]. The infectious titers (PFU/ml) are listed in Table 2.2. Finally, the number of particles that are required to produce a successful infectious event (generally visible as a plaque) was determined for each virus, resulting in the specific infectivities (PFU/particles) also listed in Table 2.2.

Less than 1% of WT particles lead to successful infection, as seen in the present results and as previously documented [55,56]. This percentage is further reduced with all of the synthetic viruses created for this study. P1-$CPB^{lo}UA^{hi}$ is particularly debilitated requiring nearly 25 times more particles than wild type to undergo a successful infection and form a plaque. The reason for the decreased infectivity of the synthetic viruses remains unclear, but this phenomenon has been documented in both codon and codon pair deoptimized viruses [27,29,52] but not in codon pair optimized PV-Max [29].

The decreased specific infectivity is reiterated when the plaque sizes of the synthetic viruses are examined. Each cell that has been successfully infected at the start of a plaque assay produces similar amounts of viral particles for all of the viruses (evidenced by Table 2.2, particles/ml). Those particles are released into their direct surroundings during incubation with tragacanth gum and have the opportunity to infect neighboring cells. Lowered specific infectivity means that fewer neighboring cells will succumb (stochastically) to infection by the synthetic viral particles and the plaques for

those constructs will be smaller in turn. This is true for P1-CG^{hi}, P1-UA^{hi} and P1-CPB^{lo}, which create medium sized plaques relative to the large plaques seen in WT after 48 hours, and especially true for P1-CPB^{lo}UA^{hi} which produces tiny plaques in the same time (Fig 2.1). These results were observed numerously, as plaque assays were conducted each time the viruses required titering. One representative image of the plaques is shown. Note that the purpose of Figure 2.1 is to point out differences in plaque size, not quantity. There is no correlation between the number of plaques displayed and the attenuation of the viruses. Rather, titers are studied in the growth curves described next.

Growth Kinetics

To determine viral growth, a single-step growth experiment with wild type or synthetic viruses was conducted by infecting HeLa cells with 10 MOI of purified virus and titering the virus by plaque assay at 0, 2, 4, 7, 10 and 24 hours post infection. A high multiplicity of infection was used in order to ensure that all the cells are infected initially, rather than infecting only a small portion of cells and allowing an additional round of infections. In this manner, the growth curve reveals information regarding the growth of the virus rather than the infectivity.

The results revealed a lower titer in all the synthetic constructs as compared with wild type poliovirus at 24 hours post infection (Fig. 2.2). The most drastic effect was seen in the two viruses containing an excess of UpA dinucleotides, namely a 20-fold and 45-fold reduction in titer as compared to wild type in P1-UA^{hi} and P1-$CPB^{lo}UA^{hi}$, respectively. In contrast, P1-CPB^{lo} and P1-CG^{hi} displayed only a 4 and 5 fold decrease from wild type, respectively.

In looking at the kinetics of the growth before reaching final titers, it is interesting that both codon pair deoptimized viruses, P1-CPB^{lo} and P1-$CPB^{lo}UA^{hi}$, displayed a delay of replication and took longer to reach their peak titers than the other viruses. While the remaining viruses have nearly peaked by 7 hours, P1-CPB^{lo} showed a sharp increase from 7 to 10 hours and P1-$CPB^{lo}UA^{hi}$ continued to increase even through 24 hours.

Summary and Discussion

In an effort to understand the effects of the generally human-suppressed CpG and UpA dinucleotides on attenuation of poliovirus by codon pair deoptimization, we have made use of a previously designed algorithm that can alter the primary sequence of a genome without altering the amino acid sequence. The algorithm shuffles existing synonymous codon pairs in order to increase or decrease the codon pair bias, and to intentionally maintain or alter dinucleotide frequencies. Here we recoded the P1 region of poliovirus with decreased codon pair bias (P1-CPB^{lo}), increased CpG dinucleotides (P1-CG^{hi}), increased UpA dinucleotides (P1-UA^{hi}), or a combination of decreased codon pair bias and increased UpA dinucleotides (P1-CPB^{lo}UA^{hi}). The purpose of designing these viruses is to decipher which characteristics are important in attenuation by codon pair deoptimization as seen in P1-Min [29] which has a low codon pair score and high CpG and UpA content.

The sequences were commercially produced in the form of cDNA and inserted into a wild type poliovirus backbone. Variant poliovirus RNAs were transcribed in vitro then transfected into HeLa cells to produce viable poliovirus. These viruses were amplified and purified to produce stocks for all subsequent experiments. Viral particle concentrations and plaque forming units were determined in the purified stocks. The ratios of these values were calculated in order to determine the specific infectivities of the viruses. The specific infectivity of WT was 1/133, showing that less than 1% of viral particles result in an infectious event.

All the recoded viruses had decreased infectivity and smaller plaque phenotypes when compared with WT, particularly P1-CPB^{lo}UA^{hi}. It has previously been shown that

the infectivity of picornaviruses is not cooperative [57], so the reduced infectivity indicates that each viral particle has a decreased probability of establishing an infection compared to a typical wild type particle. Recent evidence suggests that the specific infectivity is not related to defective virions in the particle population [53]. Although the reason for this is unclear, it is possible that the recoded viruses are defective in an early stage of infection, such as binding, uptake or uncoating.

In comparing viral titers at 24 hours post infection, P1-CPB^{lo} and P1-CG^{hi} were only four- and five-fold reduced from WT. In contrast, both viruses containing increased UpA dinucleotides were severely debilitated and only reached titers 20 (P1-UA^{hi}) and 45 (P1-CPB^{lo}UA^{hi}) fold below WT. These results provide evidence that although codon pair bias and CpG dinucleotide frequency play a role in viral attenuation, the concentration of UpA dinucleotides is a more important contributor to viral attenuation. This is in contrast to Atkinson et al [53] who found that CpG dinucleotides had a greater effect than UpA frequency in attenuation of echovirus 7.

Furthermore, the kinetics of the one step growth curve reveal an interesting feature of both codon pair deoptimized viruses. Both P1-CPB^{lo} and P1-CPB^{lo}UA^{hi} take longer to reach their peak titers than the remaining viruses, which have mostly completed viral synthesis by 7 hours post infection.

Overall, the results described in this chapter suggest that there are multiple factors leading to viral attenuation by codon pair deoptimization. The subsequent experiments aim to uncover the mechanisms by which each characteristic (codon pair score and CpG and UpA dinucleotides) affects poliovirus growth.

Chapter 2 Figures

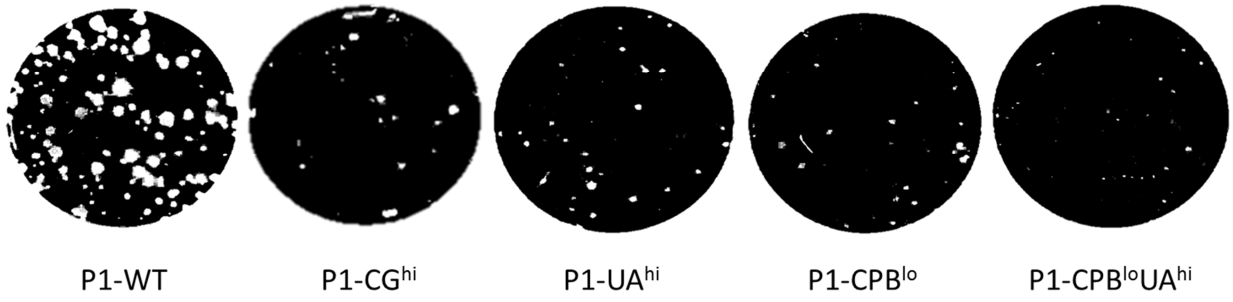

Figure 2.1: Plaque phenotypes. Plaque phenotypes of WT and synthetic viruses as seen after a 48 hour incubation with tragacanth gum at 37°C. Plaques were visualized with crystal violet stain. One representative image of the plaques is shown. Note that the purpose of the figure is to point out relative differences in plaque size, not quantity. There is no correlation between the number of plaques displayed and the attenuation of the viruses.

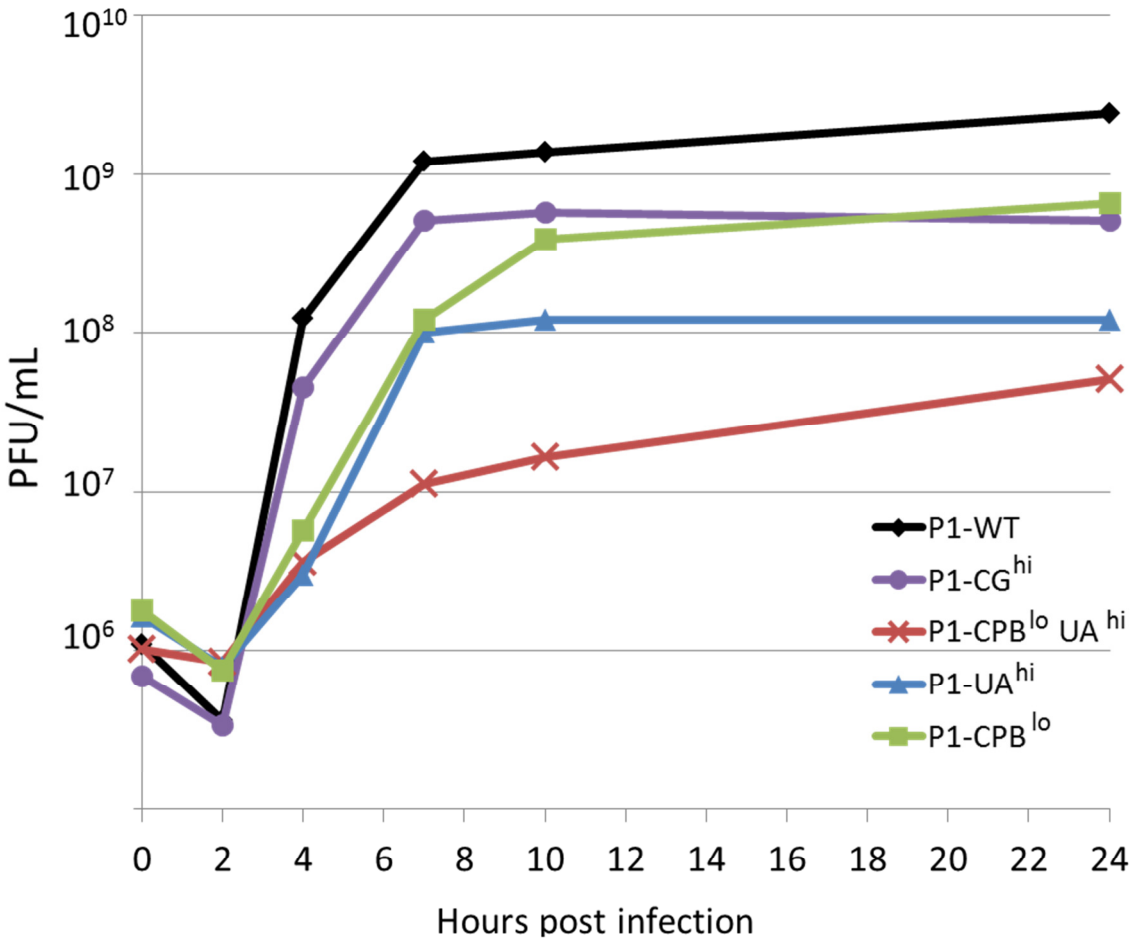

Figure 2.2: Single-step growth kinetics. One step growth curves conducted with a multiplicity of infection of 10 on HeLa cells. Results are graphed as plaque forming units per mL as determined by plaque assays. Experiment was conducted twice, with similar results both times. One representative graph is shown.

Chapter 2 Tables

Table 2.1 Codon pair bias and dinucleotide summary of synthetic viruses.

Virus	nt change from wt	CpG total	UpA total	CPB*
P1-WT	0	97	152	-0.0343
P1-CG^{hi}	629	216	129	-0.037
P1-UA^{hi}	632	97	280	-0.036
P1-CPB^{lo}	626	93	152	-0.308
P1-CPB^{lo}UA^{hi}	598	97	204	-0.307
P1-MIN	631	210	233	-0.474
P1-MAX	566	60	105	0.245
P1-SD	934	136	159	-0.095
P1-AB	680	308	282	-0.0976

*** CPB= codon pair bias**

Notes: Values shown are calculated over the entire genome, not the recoded section alone. Dinucleotide content (CpG and UpA) includes those that occur within and between codons.

Table 2.2 Specific infectivities (PFU/particle) of recoded viruses

Virus	Particles/ml	PFU/ml	PFU/particles
P1-WT	1.08E+13	8.1E+10	1/133
P1-CG^{hi}	1.02E+13	2.28E+10	1/447
P1-UA^{hi}	8.22E+12	1.14E+10	1/714
P1-CPB^{lo}	9.94E+12	1.02E+10	1/1000
P1-CPB^{lo}UA^{hi}	8.68E+12	2.64E+09	1/3284

Chapter 3: Analysis of viral protein synthesis and viral RNA replication and stability

Previous research with codon pair deoptimized pathogens has implicated translation efficiency as the cause for attenuation [29,33,34]. The current study aims to see which characteristics (codon pair bias, CpG content or UpA content), if any, are responsible for impeding viral protein synthesis and whether or not such an impediment is the source of attenuation. If so, it is also possible that insufficient viral RNA levels are the cause of the defect in protein synthesis. Both possibilities are explored in this chapter.

Viral Protein Production

In order to characterize viral protein production, HeLa cells were infected with 10 MOI of purified virus and incubated at 37°C for 5 hours. At this point, cell lysate from each infection was subjected to Western Blot for the viral protein $2C^{ATPase}$. The poliovirus genome is translated sequentially as a polyprotein that is very rapidly processed into functional proteins [12] so the concentrations of all the processed proteins are proportionate to one another. If protein synthesis is slowed at the 5' end of the genome, all the subsequent proteins will be produced in lower amounts as well. Therefore, assessing any viral protein encoded downstream of the capsid region can provide information on the rate of capsid protein synthesis. Since monoclonal antibodies which produce little background in Western blots are readily accessible for

poliovirus protein $2C^{ATPase}$, the production of this protein during infection was analyzed for all the viruses.

As seen in Figure 3.1, individually all recoded viruses produced lower levels of $2C^{ATPase}$ than wild type at 5 hours post infection. The most drastic decreases in the production of $2C^{ATPase}$ were seen in P1-$CPB^{lo}UA^{hi}$ and P1-CG^{hi} infections, which produced the protein to levels of only 61% and 67% of wild type, respectively. P1-UA^{hi} was less debilitated and produced $2C^{ATPase}$ to levels reaching 75% of WT while P1-CPB^{lo} had only a modest 12% loss (88% of wild type) of protein synthesis.

In Vivo Proxy for Rate of Viral Translation

Studying protein synthesis by infection and western blot can provide useful information on the behavior of the viruses in cell culture. However, the level of protein that is actually detected is a compilation of multiple earlier stages of infection. For example, between the start of the incubation of the virus with the cells and the time the cells are lysed, an individual virus needs to bind the CD155 receptor and have its RNA uncoated and taken into the cells. Only then is the RNA ready to be translated. If all of the recoded viruses behave identically in these early stages of infection, looking at final viral protein level can be a good readout of the rate of translation. However, we have no evidence that the viruses are comparable in these functions. Therefore, luciferase reporter constructs were used as a tool to verify the difference observed in protein synthesis in the recoded viruses while eliminating the virus' need to establish an infection.

The modified or wild type P1 regions of the viruses were cloned upstream of a Green *Renilla* Luciferase gene in a reporter plasmid such that translation would begin at the start site of the capsid protein and continue through the *Renilla* gene, resulting in a P1-Renilla luciferase (P1-RLuc) fusion protein. RNA was transcribed *in vitro* from these plasmids and a separate plasmid containing only a firefly luciferase gene (FLuc) for the purpose of an internal control (Fig 3.2A). The P1-RLuc-encoding RNA for each variant was cotransfected with an FLuc-encoding RNA into HeLa cells.

In this manner, the cells in each well translate a protein consisting of a synthetic or WT P1 fused upstream of the *Renilla* luciferase protein as well as a separate firefly

luciferase protein. Expression levels of the two luciferase proteins were assayed at 6 hours post transfection. The results are summarized in Figure 3.2B.

The trend for protein synthesis observed in this assay is similar to that seen by the Western blot method. The most drastic decreases were seen again in P1-$CPB^{lo}UA^{hi}$ and P1-CG^{hi}, both of which were reduced to about 50%. Again, P1-UA^{hi} and P1-CPB^{lo} had less drastic effects, making proteins to levels at 71% and 82% of WT, respectively.

Viral RNA Replication

The positive sense, single-stranded RNA genome of poliovirus acts as a template for viral protein synthesis and also replicates and becomes encapsidated in order to produce progeny virions. In fact, only actively translated genome RNA is subsequently accepted as template for RNA synthesis (Jiang, P*. et al*., in preparation). Genome replication, in turn, will feed genomic RNA into the translational machinery. Thus, decreased viral growth and decreased protein synthesis can both be explained by deviations in RNA levels. To address this possibility, viral RNA levels were explored by Northern blots through the course of an infection on HeLa cells with recoded viruses, specifically at 0, 4, 5, and 6 hours post infection.

In examining the RNA replication patterns of all the viruses (Figure 3.3, lanes a-d), it is interesting that both P1-CG^{hi} and P1-UA^{hi} have robust RNA replication in the first 6 hours of the infection. At the 6 hours post infection, they both appear to have replicated even better than wild type. Although this is a possibility, it is also plausible that by 6 hours the wild type virus has already encapsidated some of its new RNA and released progeny into the media (which was not analyzed in this experiment). Regardless, it is clear that RNA replication is not a limiting factor for these two synthetic viruses.

In contrast, both codon pair deoptimized viruses display a defect in RNA replication through the course of infection. P1-CPB^{lo} shows only a small accumulation of RNA by 4 hours and continues to replicate slowly through 6 hours. P1-CPB^{lo}UA^{hi} is even more incapacitated, as it shows almost no increase in RNA levels until 6 hours.

The virus has low detectable levels of RNA at 4 and 5 hours post infection, but has a comparable band at 0 hours as well (as seen in the overexposure at the bottom of Figure 3.3, lane a) suggesting that little or no replication is occurring until 6 hours later. It is noteworthy that the band seen at 0 hours in P1-CPB^{lo}UA^{hi} is a result of this virus' low specific infectivity and is not present in the wild type virus (as shown in WT overexposure). In order to achieve infection with equal MOI of WT and P1-CPB^{lo}UA^{hi}, more than 3000 times more viral particles (and therefore RNA copies) of the recoded version need to be used (see specific infectivities, Table 2.2). This is the excess RNA seen at the start of infection.

Viral RNA stability

Replication is not the sole player in controlling RNA levels during poliovirus infection. RNA stability and half-life are also important contributors. Since several of the viral constructs described here were recoded to include an excess of UpA dinucleotides, an implicated substrate for cleavage by endoribonucleases [41-43], RNA stability is a critical concern. The Northern blots described in the previous section do not account for RNA that has been degraded or that which is newly formed. It simply detects the concentration of RNA at the specific times at which the infection has been halted. To study degradation, the previous experiment was extended. In parallel to those infections already described, another set of HeLa cells was infected with equal concentrations of virus. At 4 hours post infection, these HeLa cells were treated with 2mM guanidine hydrochloride (GnHCl), a potent inhibitor of RNA replication [9]. The cells were then incubated for an additional 1 or 2 hours, at which points RNA levels were examined by Northern blotting (Figure 3.3, lanes e, f).

To determine whether or not RNA degradation is occurring, samples at 4 hours (the time at which GnHCl was added) (lane b) were compared to samples one hour after treatment with drug (lane e, 5+). This allows us to monitor the stability of RNA that has accumulated through the first four hours of infection if replication is hindered. The percent change between lanes b and e for each virus is listed to the right of the blot as determined by measuring band intensities using ImageJ.

As expected, P1-WT and P1-CG^{hi} RNA remained relatively stable after treatment with GnHCl, while P1-UA^{hi} displayed a 25% decrease in RNA levels one hour after treatment. This is consistent with previous studies which have shown increased RNA

degradation in genes with artificially high UpA content [42]. Surprisingly, RNA in samples from both codon pair deoptimized virus infections continued to increase despite the addition of GnHCl. Given that GnHCl specifically inhibits the function of poliovirus protein 2C, the lack of inhibition in these constructs might indicate that this protein is misfolded and cannot bind GnHCl. Alternatively, the viruses may have developed secondary mutations in the 2C region.

Summary and Discussion

The experiments described in this chapter aim to unravel the role of protein synthesis and the behavior of viral RNA on the attenuation of poliovirus as a result of large-scale recoding of the capsid-encoding region of the genome. Specifically, viral protein synthesis was assessed by Western blot at 5 hours post infection in HeLa cells with recoded viral variants. All of the viruses displayed decreases in the production of poliovirus protein $2C^{ATPase}$ to some extent when compared with wild type. The most drastic decreases were seen in P1-CG^{hi} and P1-$CPB^{lo}UA^{hi}$. These results were confirmed using transfection of RNA encoding luciferase fusion proteins to eliminate the possibility that the viral proteins are reduced due to the behavior of the virus early in the infection (i.e, receptor binding and uptake). The luciferase assays yielded results similar to the Western blots. Interestingly, no defined correlation can be made between efficiency of protein synthesis and viral growth or attenuation. P1-CG^{hi} showed a large decrease in protein levels but grew to levels just 5-fold lower than wild type. In contrast, P1-UA^{hi} produced proteins to levels at 72% of wild type but was attenuated 20-fold compared to wild type (Figs. 3.2 and 2.2).

These experiments detected decreased protein production but did not reveal the mechanism for the defect. Decreased protein levels can be a result of slowed rate of translation due to specific characteristics in the RNA, such as secondary structure [58,59] or the interactions of tRNA during synthesis. Alternatively, the proteins may be misfolded and signaled for degradation by the cellular machinery [60]. Both possibilities would result in lower net protein production but they are not exclusive of one another. It is plausible that a slowed rate of translation can alter protein folding. To see if codon

pair deoptimized viruses have slowed translation and if ribosomes are stalling on the messenger, ribosome profiling assays are currently underway in the lab. It is expected that these experiments will provide clarity as to what RNA characteristics are involved in decreasing viral protein synthesis in recoded viruses.

Thus far, the results described here show that codon pair score alone does not signal a strong effect on viral protein synthesis. P1-CPB^{lo} produced protein levels at 80% and 88% of wild type in luciferase assays and western blot, respectively. However, when codon pair deoptimization is combined with increased UpA dinucleotides (P1-CPB^{lo}UA^{hi}), the effect is drastic.

Because UpA dinucleotides have been implicated in RNA degradation, it was important to analyze the behavior of viral RNA through the course of infection. While the rest of the viruses displayed robust RNA replication from 4 to 6 hours post infection, both codon pair deoptimized viruses (P1-CPB^{lo} and P1-CPB^{lo}UA^{hi}) showed severe delays in RNA accumulation. This coincides with data in the previous chapter which shows that growth in these constructs is delayed during the early time points of infection (i.e. 4 hours pi, Figure 2.2). Interestingly, the inability to accumulate RNA during this time does not mean that the virus is destined to severe attenuation. P1-CPB^{lo} eventually reaches titers less than 4 fold lower than wild type. The mechanism by which the virus recuperates is unclear, but it is possible that the codon pair deoptimized viruses exhibit slowed RNA replication or are defective at internalizing the viral genome. This can mean that internalization takes longer than WT or that fewer genomes are actually successful at entering the cell. However, once inside the cells, the genomes of P1-CPB^{lo} are eventually replicated to the cell's capacity. These results suggest that

RNA replication and codon pair deoptimization (without increased UpA and CpG dinucleotides) have only modest effects on attenuation of poliovirus.

P1-CPB^{lo}UA^{hi} is not as successful in recovering from the lack of accumulation early in the infection, likely hindered by its high UpA content. To determine if increased UpA dinucleotides confer decreased RNA stability due to cleavage by endoribonucleases, infected cells were treated with an inhibitor of viral replication (guanidine hydrochloride). P1-UA^{hi} was the only virus in which a decrease in RNA was visible. In fact, two of the viruses (P1-CPB^{lo} and P1-CPB^{lo}UA^{hi}) had drastic increases in RNA despite the addition of the inhibitor. This may be representative of improper folding of viral protein 2C^{ATPase} which therefore could not be bound by GnHCl. It is noteworthy that had P1-CPB^{lo}UA^{hi} been entirely susceptible to the drug, degradation was expected in the RNA of this virus as well. Polioviruses resistant to inhibition by GnHCl have been described before [9] and this trait of the P1-CPB^{lo} and P1-CPB^{lo}UA^{hi} is currently under further investigation.

Interestingly, there is no correlation between levels of viral RNA in the cell and the production of viral proteins, as evidenced by the behavior of two viruses in particular: P1-CPB^{lo} and P1-CG^{hi}. P1-CPB^{lo} accrued very little RNA compared to WT by hours post infection, but had produced concentrations of protein very similar to WT. Upon entrance into the cell, the poliovirus genome is first translated in order to produce proteins that are essential for replication. It is clear from this data that very little RNA is required to produce all the proteins that the virus will eventually use. In contrast, P1-CG^{hi} produced very high levels of stable RNA in this study, but displayed a defect in translation as determined by both Western blot and luciferase assays. Previous studies

have shown that genes artificially enriched for CpGs confer increased RNA stability as compared with wild type [43]. The mechanism(s) stabilizing the RNA is not clear but the increased CpG dinucleotides may be reinforcing the structure of the RNA thereby slowing the progression of ribosomes along the RNA and reducing the overall rate of protein synthesis as previously suggested [43,59]. The ribosome profiling assays currently underway in our lab are expected to ascertain the validity of this hypothesis. If it is accurate, the increased RNA stability is counterproductive and may be the reason for the slight attenuation seen in P1-CG^{hi}.

Chapter 3 Figures

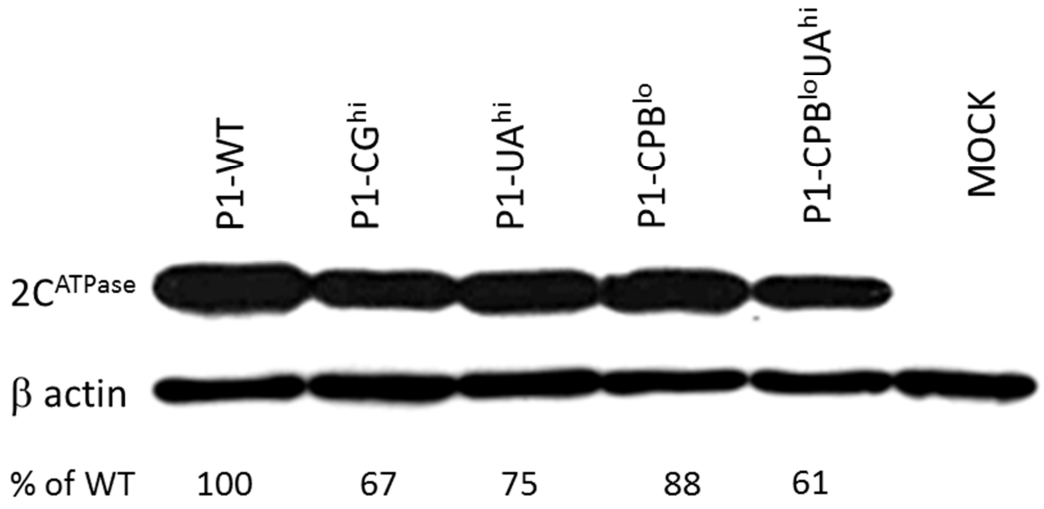

Figure 3.1: Poliovirus protein 2C^{ATPase} detection. Western Blot for poliovirus protein 2C^{ATPase} and internal control β actin in HeLa cells infected with 10 MOI of each virus. Cell lysates were analyzed at 5 hours post infection. Following detection of 2C bands, the membrane was stripped and probed for the internal control β actin. Band intensities of 2C^{ATPase} were normalized to β actin and expressed as a percentage of WT. One representative image is shown.

A

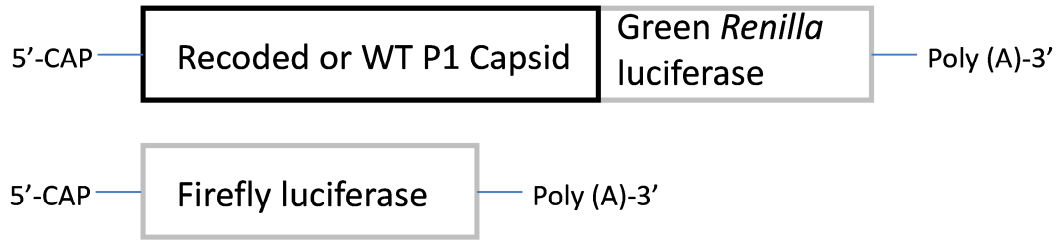

B

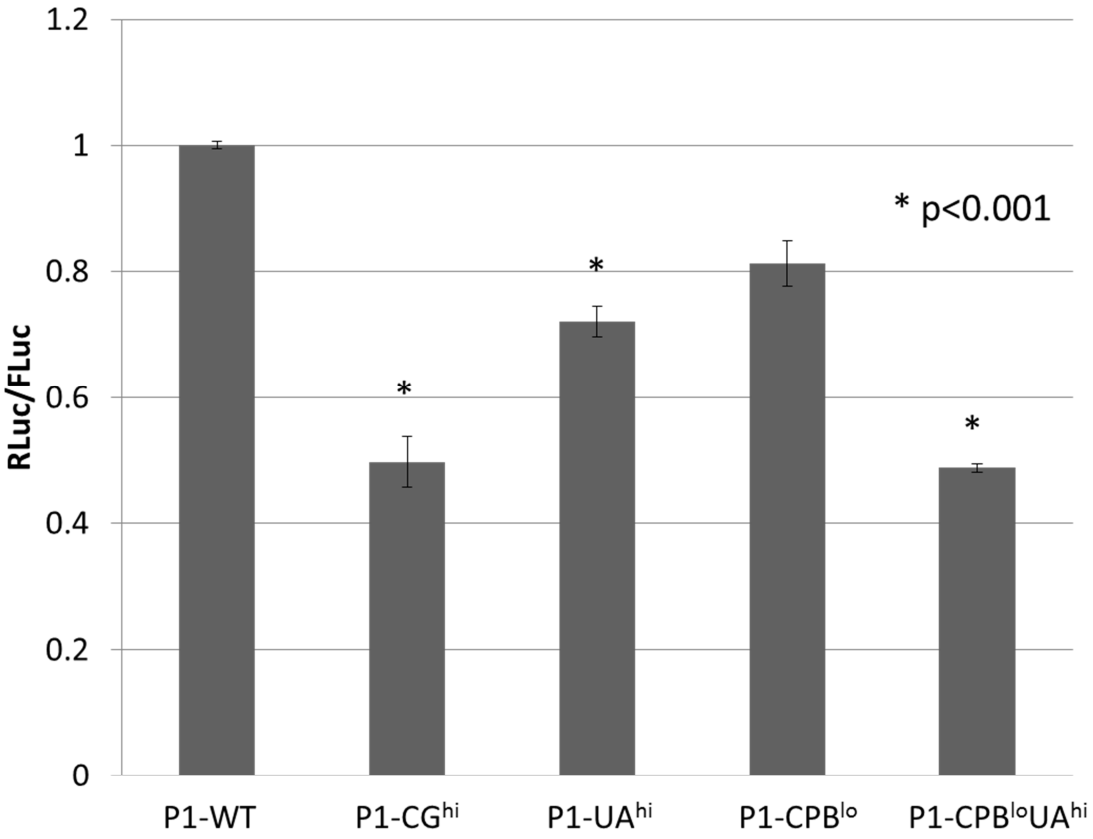

Figure 3.2: Analysis of translation using luciferase reporter plasmids. (A) Diagrams of RNA transcribed from plasmids containing recoded P1 regions cloned upstream of the Green *Renilla* luciferase gene and an internal control expressing the firefly luciferase gene. .The capped RNAs are cotransfected into HeLa cells and assessed for luminescence 6 hours post transfection. (B) *Renilla* and firefly luciferase levels were analyzed and their ratios were graphed as a representation of P1 translation levels. Results are the average of triplicate transfections. (*) represents statistical significance of p<0.001 using the student's t test.

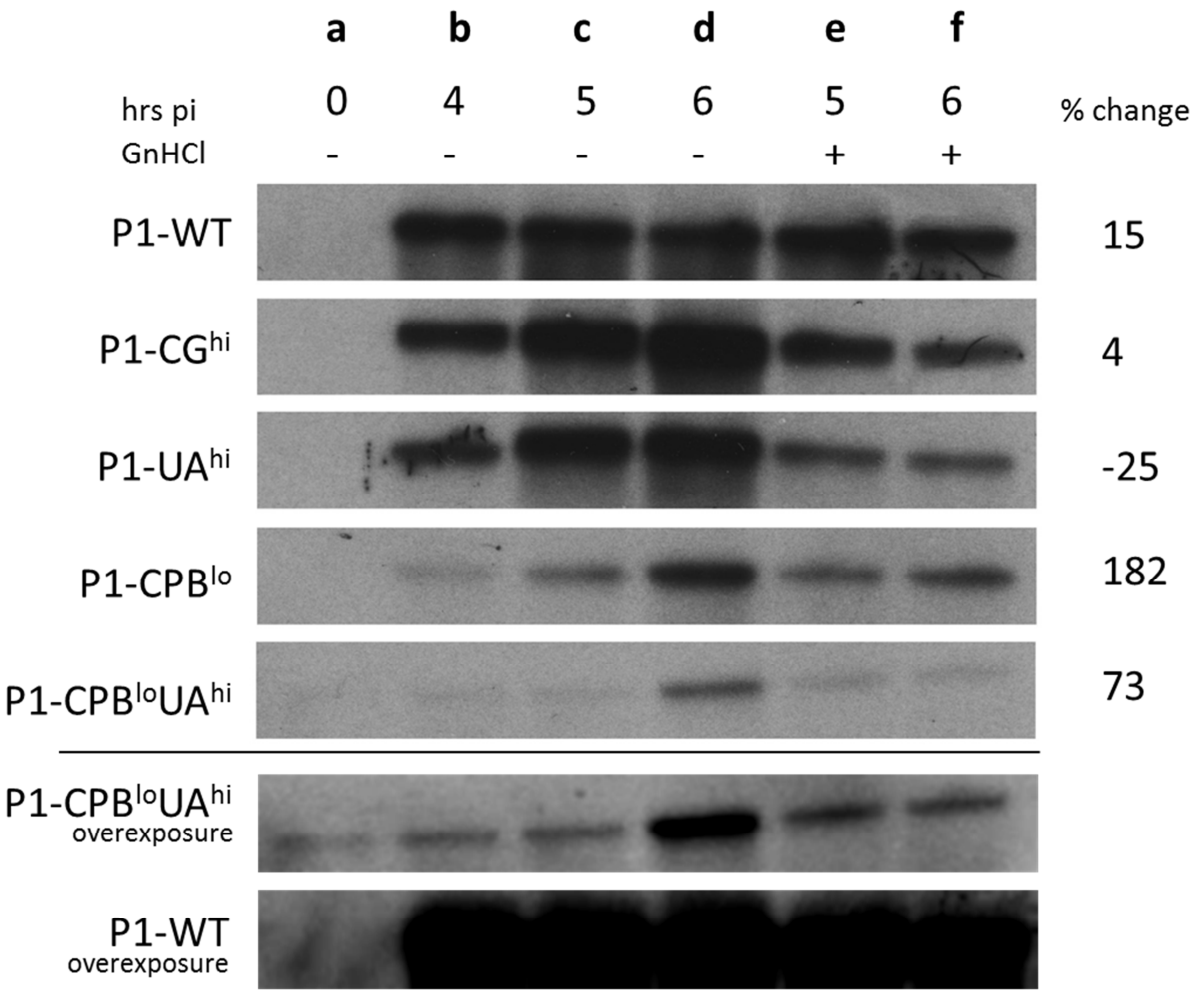

Figure 3.3: Measurement of RNA levels in cells infected with recoded viruses. RNA accumulation was followed by Northern blots using a probe against positive strand PV RNA. RNA samples were extracted from cells infected with various viruses at 10 MOI. Columns a-d show RNA levels in lysates at 0, 4, 5, and 6 hours post infection in the absence of guanidine hydrochloride. Columns e-f show RNA levels in lysates from parallel infections at 5 and 6 hours where GnHCl was added to media at 4 hours post infection. Band intensities were determined by ImageJ. The percent change in RNA from 4 hours to 1 hour later, after the addition of GnHCl (5+, column e), is listed on the right. Overexposure of P1-$CPB^{lo}UA^{hi}$ is shown in order to visualize the high concentration of input RNA (0 hr) as compared with wildtype. This particular experiment was not normalized with an internal control. However, a separate repetition showed a similar trend with approximately equal loading concentrations as determined by probing for GAPDH. Data is not shown due to poor resolution of film as a result of inefficient membrane stripping.

Chapter 4: Influence of CpG dinucleotides on innate immune response in cell culture

Unmethylated CpG dinucleotides have been shown to trigger the innate immune system by various pathways [47-50]. Since vertebrate genomes strongly suppress CpG dinucleotides, the RNA viruses which infect those vertebrates may have evolved similar suppression such that the viral genome is more difficult to detect and eliminate by the host cell. The possibility remained that viruses containing artificially high CpG dinucleotides (such as P1-Min and P1-CG^{hi}) were more susceptible to clearance by the cell due to an increased innate immune response. Type I interferons are one of the major cytokines produced in response to a viral or bacterial infection. Therefore, the interferon response to infection with P1-CG^{hi} in HeLa cells was compared to that of WT.

Type I IFN protein production

Infections in HeLa cells with WT or P1-CG^{hi} were carried out as described in earlier chapters, with 1 or 10 MOI of each virus, including a mock infection and transfection with Poly I:C as a positive control. Poly I:C is a dsRNA analogue known to induce an interferon response [61]. The infections were allowed to proceed for 4, 8, or 12 hours (IFNα) or 2, 4, and 6 hours (IFNβ) at which point supernatant was collected and analyzed by ELISA using Antigenix America Inc. cytokine ELISA kits for human IFNα or β. The ELISAs were carried out according to the manufacturer's instructions in duplicate samples. Final results are summarized in Figures 4.1 (IFNα) and 4.2 (IFNβ).

As seen in Figure 4.1, cells infected with both variants of poliovirus stimulated the production of interferon alpha whereas mock infected cells did not. It is likely that the infected cells produced a lesser response than those in the positive control because poliovirus has evolved mechanisms to evade the innate immune response [62,63]. In contrast, neither variant of poliovirus was capable of stimulating interferon beta production (Fig. 4.2). This is not surprising despite the slight stimulation of IFNα because different pathways are used to stimulate the two type I interferons. Poliovirus may be more adept at inhibiting the pathway for the production of IFNβ.

Importantly, there was no apparent difference in the induction of type I IFN proteins seen between WT and P1-CG^{hi}, indicating that CpG dinucleotides are not more immunostimulatory under these conditions.

Analysis of IFNβ RNA and transcription factors

IFNβ RNA production

Although there was no apparent induction of IFNβ protein production, it was still possible that IFNβ RNA was being transcribed in these cells but was not subsequently translated. To address this, HeLa cells were infected with P1-WT, P1-CG^{hi}, Newcastle Disease Virus (a negative strand virus known to be a strong inducer of interferon; which served as a positive control), or mock infected in duplicates. RNA was extracted from the cell lysates and was subjected to quantitative RT-PCR in order to determine the production of IFNβ RNA. Results were normalized to concentrations of GAPDH RNA (a loading control) then expressed as fold-change from mock infection (Fig 4.3). According to these results, there is no change in IFNβ RNA levels during infection with P1-WT and P1-CG^{hi} under the given conditions.

IFNβ promoter activation

As a final confirmation that this cytokine is not being induced, a reporter plasmid was used to assess any transcription factors that would induce the IFNβ promoter in a cell. The plasmid (depicted in Figure 4.4A), which contains a firefly luciferase reporter gene under the control of an IFNβ promoter sequence, was transfected into HeLa cells overnight along with a plasmid containing the *Renilla* luciferase gene to serve as an internal control. The following morning, the cells were infected with 10 MOI of P1-WT or P1-CG^{hi} virus in triplicates. Five hours post infection, the supernatants from infected cells were analyzed for luciferase activity. Results are shown in Figure 4.4B as a ratio

of firefly to *Renilla* luciferase. The lack of significant change from mock infected cells indicates that no activation of IFNβ was detected in the wells infected with either virus.

Summary and Discussion

Poliovirus produces long double-stranded RNA during replication, making it a likely candidate for eliciting an innate immune response via the MDA5 receptor [64]. Additionally, unmethylated CpG dinucleotides have been implicated in stimulation of the innate immune response repeatedly [47-50], likely because they are recognized by the host as non-self genetic material. Poliovirus genomes, however, just like many vertebrate viruses, is deficient in the expected frequency of CpG dinucleotides [39,40,65]. Therefore, a potential source for the differences seen in growth between wild type poliovirus and P1-CG^{hi} is variability in the immunogenicity in cell culture. For example, an increased type I interferon response caused by the synthetic virus may contribute to its attenuation. To address this, the interferon α and β responses were measured by ELISA in supernatants from HeLa R19 cells at various time points post infection using poly I:C, a dsRNA analog known to induce an interferon response, as a positive control. According to the data in figure 4.1, there was a modest increase of IFNα in infected cells in comparison with mock infection but there was no significant difference in the protein levels between the two viruses. The concentration of IFNβ protein in the infected cells did not vary significantly from a mock infected culture or from one another (Fig 4.2).

Despite the lack of IFNb protein production, it was still possible that IFNb RNA was being transcribed in poliovirus infected cells, Therefore, IFNβ mRNA production in infected HeLa cells was examined by quantitative real time PCR at various time points post infection using New Castle Disease virus as a positive control. Once again, there was no significant change in IFNβ RNA levels from mock infected cells (Fig 4.3).

Similar results were obtained using a reporter plasmid which uses the IFNβ promoter to activate translation of the firefly luciferase gene (Fig 4.4). These results conflict with previously published data that detected a transcriptional IFNβ response as a result of wild type poliovirus infection [62], although a different strain of HeLa cells was used, which may be a cause for the discrepancy.

Nonetheless, it is conclusive that the type I interferon response does not play a role in the attenuation seen in PV-CG^{hi}. The increased CpG content in this virus does not seem to directly or indirectly influence immunogenicity as thought, nor does the slower growth allow a more robust build-up of the cytokines in question.

Chapter 4 Figures

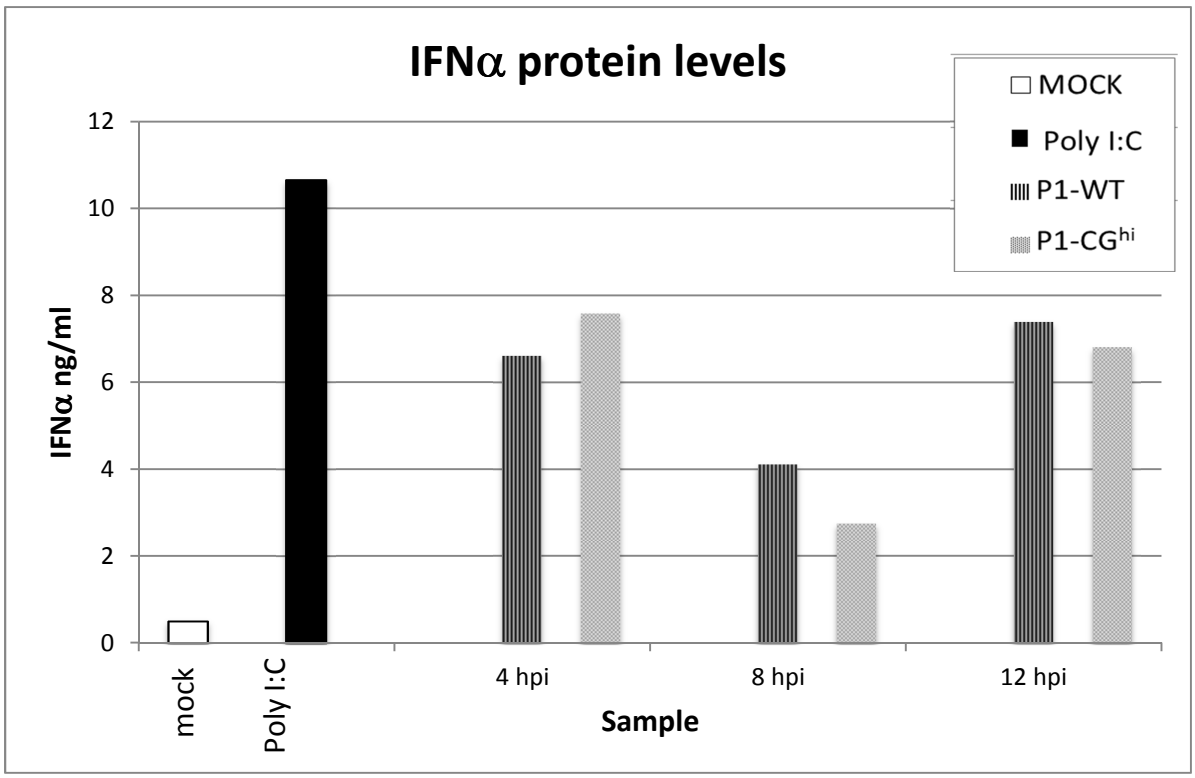

Figure 4.1: IFNα protein production in infected cells. Supernatants of cells infected with 10 MOI of virus were subjected to ELISA for IFNα protein quantification. Protein concentration was extrapolated using absorbency readings and a standard curve. Poly I:C was used as a positive control. Results are the averages of readings from duplicate samples.
*hpi= hours post infection

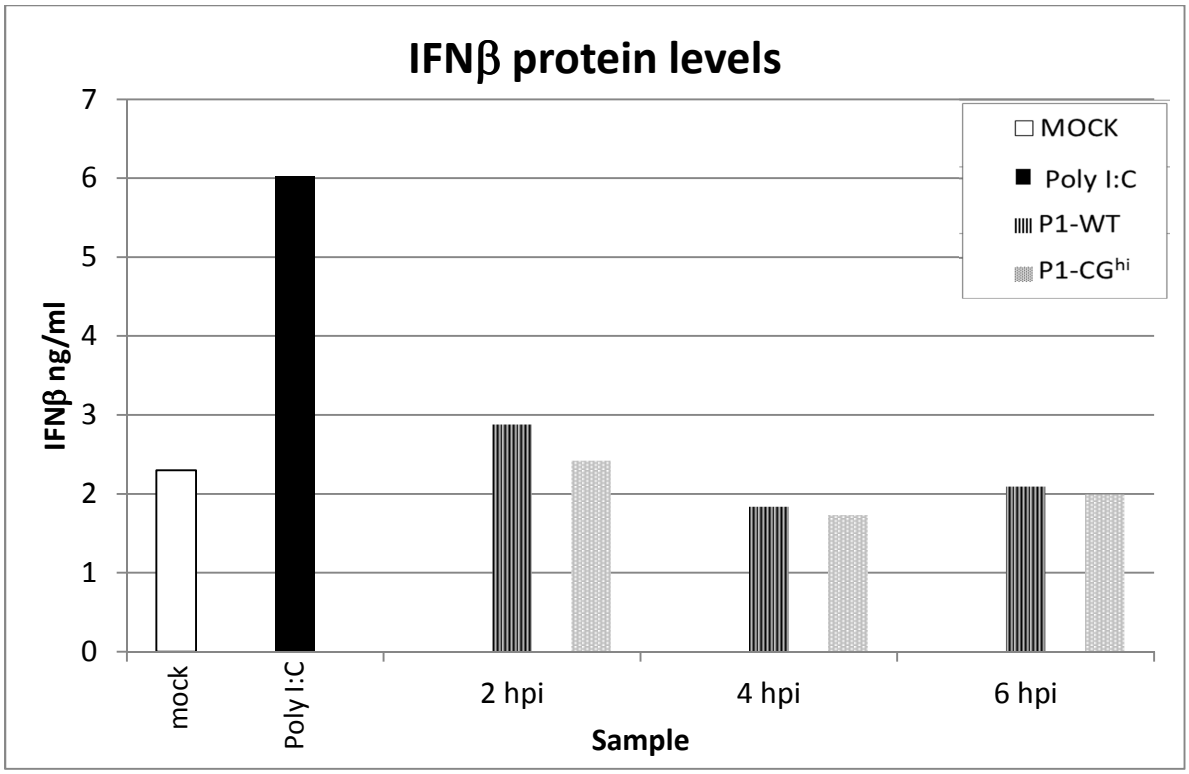

Figure 4.2: IFNβ protein production in infected cells. Supernatants of cells infected with 1 MOI of virus were subjected to ELISA for IFNβ protein quantification. Protein concentration was extrapolated using absorbency readings and a standard curve. Poly I:C was used as a positive control. Results are the averages of readings from duplicate samples.
*hpi= hours post infection

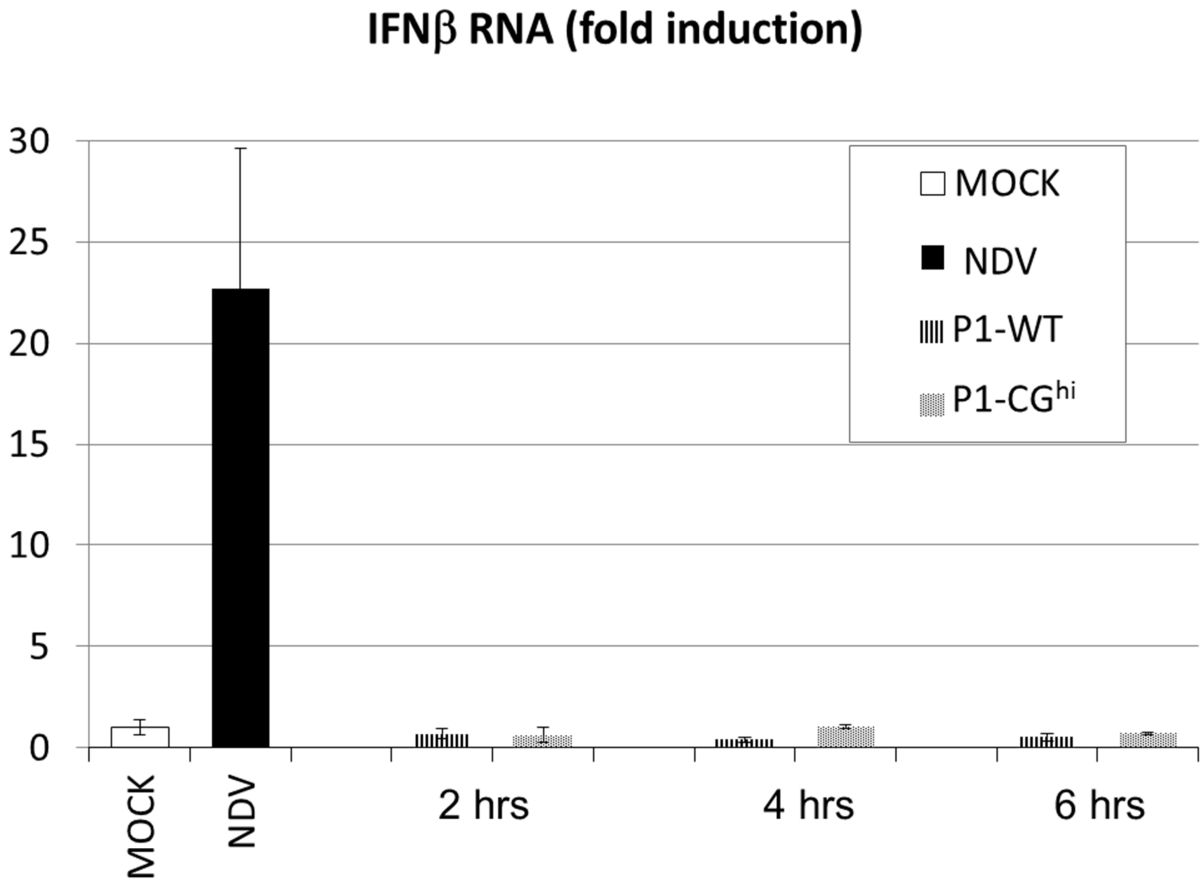

Figure 4.3: IFNβ RNA expression in cells infected with recoded viruses. Cells were infected with an MOI of 3 of WT or P1-CG^{hi} viruses and total RNA was extracted at various times post infection. Levels of IFNβ RNA were analyzed by qRT-PCR and normalized to the endogenous control GAPDH. Values are expressed as fold change from a mock infected plate using the $\Delta\Delta C_T$ method. Newcastle Disease Virus (NDV) was used as a positive control for interferon induction. Results are shown as the averages of triplicate samples.

A

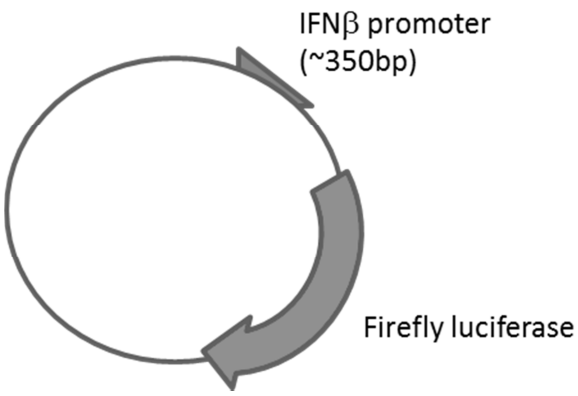

B

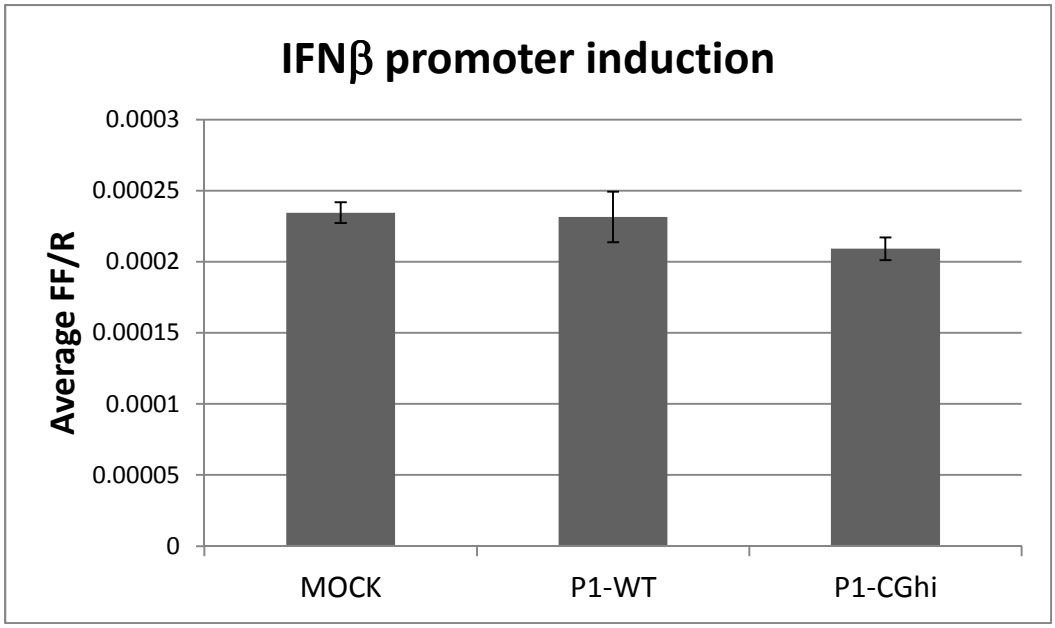

Figure 4.4: Measurement of IFNβ promoter induction. (A) Diagram of plasmid used to measure transcription factors responsible for activation of IFNb production. This plasmid and another that contains only a *Renilla* luciferase gene were transfected into HeLa cells prior to infection with virus. (B) Cells harboring the luciferase plasmids were infected with 10 MOI of virus and analyzed for luciferase activation 5 hours post infection. *Renilla* luciferase production was used as a control for transfection efficiency so the results are shown as a ratio if firefly to *Renilla* activity. Results are the averages of triplicate infections.

Chapter 5: Neurovirulence of Attenuated Virus

One of the major reasons it is important to discern the effects of the different characteristics of codon pair deoptimization is to boost the utility of this procedure for vaccine development. The ability to quickly assemble an attenuated version of a virus is invaluable in the event of an emergent pandemic or bioterrorist attack. If the attenuating effects of varying features of the genetic code are understood, any virus can quickly be designed and produced. Today, it is possible to have DNA fragments of up to 3kb synthesized commercially in under two weeks, and that turnover is likely to be even shorter in future years as technology advances.

This method of codon pair deoptimization and chemical synthesis can also be used to improve on vaccines that already exist. For example, since the implementation of The Polio Eradication & Endgame Strategic Plan by the World Health Organization, there has been a pressing need for novel vaccine candidates to eliminate the occurrence of cVDPVs in populations that are poorly immunized. Additionally, recent statistics show that the current influenza vaccines (flu shots) have poor efficacy in those populations who are most susceptible to complications due to infection with influenza. Although the overall effectiveness in healthy adults under the age of 65 is near 90%[66], the populations of elderly over the age of 65 and of children over the age of two have shown only 58% [67] and 59% [68] efficacy, respectively. Furthermore, studies in infants and toddlers aged 6 to 23 months have revealed efficacy as low as 49%[69]. A contributing factor to low effectiveness in these groups is mismatched antigens since

the expected seasonal flu strains need to be determined far enough in advance for manufacturing. Evidence shows that in some seasons mismatched strains can provide reduced but substantial cross-protection against drifted strains in healthy adults, which promotes the high efficacy in that population[70].

Finally, many viruses exist that do not have vaccines at all. Codon pair deoptimization can provide a novel platform in the right direction to creating vaccine candidates. This includes vaccine development for animals, particularly those agriculture animals who live in herds and easily spread life-threatening infectious disease. The health of these animals plays an important role on the country's economy.

All of these potential uses of codon pair deoptimization for vaccine development make it an important phenomenon to clearly understand. Although work has already been published that shows that codon pair deoptimized viruses are attenuated in animal models [29], the attenuated P1-CPB^{lo}UA^{hi} virus described here also had potential for drastic decreased neurovirulence due to its slowed replication. It was hypothesized that the virus would be weak enough to elicit an immune response and be cleared by the animal before it had a chance to overcome the nervous system.

Neurovirulence of P1-CPB^{lo}UA^{hi} in susceptible animal model

Neurovirulence of P1-CPB^{lo}UA^{hi} was tested in mice transgenic for the poliovirus receptor CD155 (*CD155tg* mice), which are susceptible to infection with poliovirus via the intradermal, intramuscular, intravenous or intracerebral routes (but not via the oral route) [31]. Three independent experiments were conducted in which groups of 4 mice, aged 6-8 weeks, were anesthetized and injected intracerebrally (i.c.) with 10^4,10^5,10^6, or 10^7 particles of P1-WT or P1-CPB^{lo}UA^{hi}. These doses were chosen because they are lethal and sublethal doses of wild type virus. All mice were monitored daily for 21 days and euthanized at first signs of paralysis.

The fifty percent lethal dose (LD_{50}) was calculated by the Reed-Muench method[71]. In contrast to the drastic attenuation that is seen with P1-CPB^{lo}UA^{hi} in cell culture studies, the average LD_{50} for P1-CPB^{lo}UA^{hi} ($2.26x10^5$ particles) was only tenfold higher than wild type ($2.37x10^4$ particles).

A successful vaccine candidate must have a broader safety zone so further vaccination studies in animal models were not conducted with this virus. However, it is possible to generate versions of codon pair deoptimized viruses that are more attenuated and have a larger safety zone. For example, subclones of PV-Min had LD_{50} values that were up to three logs higher than wild type [29]. Such attenuated viruses would also be appropriate to use as seed viruses for inactivated vaccines because they are safer than their wild type counterparts. A particularly successful case of viral attenuation by CPD is the recoded influenza virus (NA+HA)(Min). Here the LD_{50} is $\geq 3.16\times10^6$ PFU, which is about 100,000-fold higher than its wild type parental strain PR8 [33].

In addition to the substantial work that has already been done using influenza A virus, studies can be extended to apply aspects of codon pair deoptimization to other viruses that do not already have vaccines with high efficiency. For example, work with Dengue virus and Vesicular Stomatitis Virus (VSV) is currently underway in the lab. Now it is possible to recode the viruses with particular goals in mind, such as decreased protein synthesis, slowed genome replication, or decreased messenger half-life.

Chapter 6: Fitness assessment for previously described poliovirus variants

Previous work in the lab has shown that two synthetically redesigned polioviruses, PV-SD (in which the codons in the P1 region of the genome have been randomly shuffled) [27] and PV-Max (in which the codons in the P1 region have been reorganized to maximize the codon pair bias) [29] behave similarly to wild type poliovirus in cell culture and in animal models. In order to analyze the fitness of these viruses as compared to wild type in cell culture, the synthetic viruses were put through a series of passages in competition with wild type. In this case, the fitness of a specific virus is defined by the extent to which it can multiply under defined conditions. Two viruses that are co-infecting host cells compete not only for cell surface receptors but also for numerous host cells factors. If one of the viruses displays a disadvantage at particular stages of infection, it will be clear in competition assays even if the defect was not apparent during infection with that virus alone.

Competition Assays

The synthetic (PV-SD or PV-Max) and wild type polioviruses were used to coinfect HeLa cells using an MOI of 5for each virus. At this MOI, most cells will obtain at least one infectious unit of each virus. Infections were carried out as described above and were allowed to proceed for 24 hours. Cell debris was cleared and the resulting virus pool (now a combination of PV-SD and WT or PV-Max and WT) was

titered by plaque assay and was subsequently used to infect a naïve monolayer of HeLa cells with a combined MOI of 10 in the same manner. The viruses were passaged as such ten or more times. At given intervals, the total RNA was harvested from the cells and subjected to quantitative RT-PCR using primers specific to each virus and primers specific for GAPDH mRNA to serve as an internal control (Table 6.1).

Although on its own PV-SD showed growth kinetics similar to wild type, when subjected to competition against wild type it proved to be less robust. By the sixth passage there was no detectable RNA from PV-SD, whereas the wild type RNA was abundant (Figure 6.2). These results suggest that PV-SD is slightly attenuated, but this attenuation is too minor to detect in its growth on its own. When the virus is suddenly exposed to coinfection, this slight defect is exaggerated with each passage due to competition for resources. It is not surprising that PV-SD displays a phenotype because it has a modest decrease in codon pair bias and an increase in CpG dinucleotides (see Table 2.1), two features that have herein been shown to cause slight attenuation. In contrast, the ratio of PV-Max to wild type fluctuated near 1 (Figure 6.2), indicating that the viruses do have nearly identical fitness.

Chapter 6 Figures

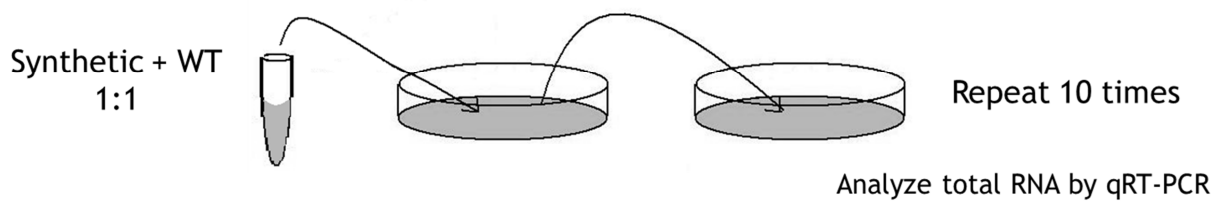

Figure 6.1: Schematic of competition assays. Synthetic (PV-SD or PV-Max) viruses were combined with wild type in equal concentrations and were used to infect HeLa cells such that the combined MOI was 10. 24 hours later, the supernatant was titered and then used to infect naïve cells at an MOI of 10. This was repeated 10 times, and the concentration of RNA for each virus was determined by qRT-PCR at set intervals.

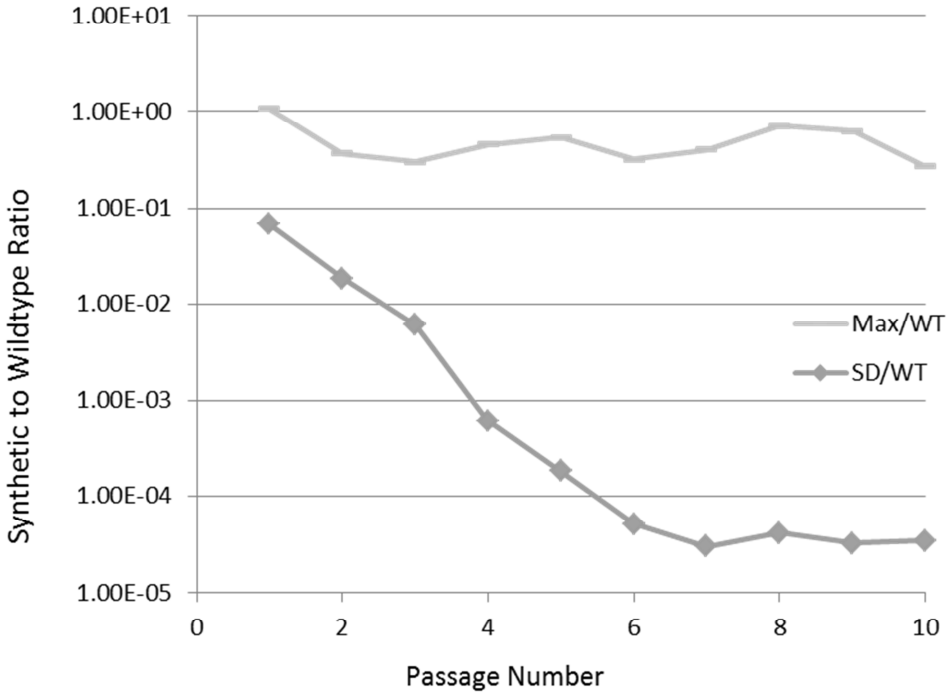

Figure 6.2: Ratios of synthetic to WT viruses after competition. Ratios of qRT-PCR data were plotted such that the concentration of the synthetic virus is shown relative to WT. One set of passages was subjected to duplicate RNA analysis. The results plotted on the graph are averages of the two analyses. Diamond data points represent PV-SD while the dashed data points represent PV-Max.

Chapter 6 Tables

Table 6.1: Primers used for qRT-PCR in competition assays.

WT/SD competition primers	
PV-SD (fwd)	5’ GAAAGAAGCTATGCTTGGGACC 3’
PV-SD (rev)	5’ GTCCCTTAGGAGCCTGACTG 3’
PV-WT1 (fwd)	5’ GCGTAAGGAGGCGATGTTG 3’
PV-WT1 (rev)	5’ GGTATCTCGCAACAAGCGC 3’
WT/Max competition primers	
PV-Max (fwd)	5’ GACAAGAATTGTGGTGCCG 3’
PV-Max (rev)	5’ CGAAGCCTCTGTATTTGGC 3’
PV-WT2 (fwd)	5’ CGTCCCTCTTTCGACACCC 3’
PV-WT2 (rev)	5’ CTGGCTTCAGTGTTTGGGAG 3’
GAPDH primers	
GAPDH (fwd)	5’ GGAAGGTGAAGGTCGGAGTCAACGG 3’
GAPDH (rev)	5’ TCCTGGAAGATGGTGATGGGATTTC 3’

Chapter 7: Discussion and Future Directions

Discussion

Codon pair bias, the preferential pairing of certain codon pairs over others, is a complex phenomenon that is poorly understood. The advancement of synthetic biology has made it possible to study this phenomenon to a greater extent than ever before. A specially designed computer algorithm is capable of shuffling the existing codons of a gene in order to codon pair optimize (include mostly overrepresented codon pairs) or codon pair deoptimized (include mostly underrepresented codon pairs) the sequence without altering the amino acid sequence or the codon usage. These DNA fragments can be commercially manufactured with relatively fast turnover- for example, synthesis of a 3kb sequence can be completed in under 3 weeks.

Previous research has indicated that codon pair optimizing the capsid sequence of poliovirus had little to no effect on viral growth, while codon pair deoptimizing the same sequence rendered it inviable [29]. Notably, when smaller segments of the deoptimized region were subcloned into a wild type backbone, the resulting viruses were viable but severely attenuated. Although the reason for this phenomenon is unclear, it is evident that increasing underrepresented codon pairs in an RNA virus coding region consequently increases the frequency of CpG and UpA dinucleotides. These dinucleotides are suppressed in a variety of species and may be responsible for attenuation by codon pair deoptimization. The goal of the current study was to determine the effects of CpG and UpA dinucleotide frequencies on viral attenuation by codon pair deoptimization.

The results described here characterize four newly designed and synthesized variants of poliovirus. These variants have been recoded to include specific features of codon pair deoptimization: codon pair bias, CpG dinucleotides, UpA dinucleotides or a combination of codon pair bias and UpA dinucleotides. Changes were made in the capsid region (P1) of poliovirus by shuffling existing synonymous codons such that the amino acid sequence and codon usage remained unaltered.

Analysis of single-step growth kinetics shows that increased UpA dinucleotides are the most influential aspect of codon pair deoptimization since the two viruses with increased UpA content were most attenuated (20-fold and 45-fold at 24 hours post infection). Analysis of RNA stability provided evidence that UpA dinucleotides in RNA are favored to be degraded and decrease the half-life of the mRNA. Decreased RNA stability may be the mechanism for viral attenuation in the high UpA viruses.

In contrast, the virus containing only a high concentration of CpG dinucleotides was less than 5-fold attenuated in growth experiments in HeLa cells, suggesting that although CpG content may have a small contributing effect to attenuation by codon pair deoptimization, it is not a strong determinant of viral growth. Since unmethylated CpG dinucleotides have been implicated in stimulating innate immunity, experiments were conducted to assess the effect of increased CpG content on immunogenicity. No differential induction of type I interferons was detected. The genome of this CpG-rich virus also replicates well in cell culture, leaving the apparent compromised protein synthesis as the main culprit for the minor attenuation seen in this virus. However, in

general, translation efficiency does not seem to be a major determinant of viral growth and spread.

These results are supported by research published by two independent groups. Burns *et al* [51] reported decreased viral infectivities in poliovirus variants that contained increased CpG or UpA dinucleotides in the capsid sequence while maintaining codon bias. The group also attempted to analyze the effect of increasing CpG and UpA content without altering codon pair bias. However, the construct they created had a different codon usage than wildtype rendering it an inadequate resolution to the dinucleotide content versus codon pair bias question. In contrast to the results described here, Burns *et al* reported no change in translation efficiency of the recoded and attenuated viruses [51]. It is likely that that reason for this is that they did not use assays that were as sensitive to slight differences in translation levels as the ones described herein. They show only ^{35}S labeled poliovirus proteins, which can easily detect problems with proteolytic processing, but does not adequately assess relative differences in concentrations of specific proteins.

More recently, the second group, Atkinson *et al* [53], show that viral infectivities decreased with increased CpGs and UpAs in a related picornavirus, echovirus 7, when altering dinucleotide content. Moreover, they showed that decreasing CpG or UpA content enhanced viral replication and increased plaque size. Although many of the findings in their results are similar to the ones described here, Atkinson *et al* found that CpG dinucleotides are more influential in attenuation than UpA dinucleotides [53]. It is possible that the context (such as virus, host cell, region of deoptimization) into which the excess dinucleotides are placed plays a role as to the effect they will exert.

It is noteworthy that both studies, Burns *et al* [51] and Atkinson *et al* [53], addressed dinucleotide content without entirely separating it from both codon bias and codon pair bias. The experiments described here are the first to adequately describe the effect of codon pair bias when it is separated from codon bias and CpG and UpA frequencies. The results reveal that codon pair bias alone seems to affect RNA replication although it is unclear why. Both viruses with low codon pair biases exhibited decreased levels of RNA, particularly around 4 and 5 hours post infection. The growth curves mirror this phenomenon but provide evidence that the lag can be overcome as the infection proceeds. Additionally, this defect does not correlate to decreased translation and is not a determinant of attenuation unless it is combined with increased UpA dinucleotides.

In conclusion, viral attenuation by codon pair deoptimization is a complex pattern and is combination of multiple features which have different effects on the behavior of the virus. According to the results described here, the most important attenuating feature is increased UpA dinucleotides, likely due to decreased RNA stability. Decreased codon pair bias has a slighter attenuating effect, primarily early in infection and mostly recovers later in infection. Finally, increasing CpG dinucleotides slightly decreases the final titer of the virus, likely due to compromised protein production. Most importantly, these features have an additive effect and can be combined to create more attenuated viruses as is seen with the virus described herein which contains a low codon pair bias and a high UpA concentration and with the previously described PV-Min [29].

Future Directions

Although the codon pair bias phenomenon is beginning to be unraveled, there is still much work to be done in order to fully understand the effects that it exerts on a genome. One major question to pursue relates to the lag of RNA replication during infection with codon pair deoptimized variants of poliovirus. It is likely that these variants are deficient in an event upstream of replication during infection. This event can be any of the hurdles that a virus needs to overcome at the initial stages of infection, such as receptor binding, viral uptake, or RNA uncoating. In fact, a recent study provided evidence that modifications in the codon usage of the capsid coding region of Hepatitis A correlated to changes in capsid conformation and affected viral entry and uncoating [72].

One way to address these early steps in infection is to make use of fluorescent labeling. Specifically, Syto82 is a fluorescent nucleic acid intercalating dye that is membrane permeable, noncytotoxic and does not interfere with RNA incorporation into virions [4]. When introduced to HeLa cells during infection with poliovirus (and poliovirus variants, in this case) the dye will bind to newly replicated viral RNA and get incorporated into the maturing virus particles. These RNA-labeled viral particles can then be used in combination with typical immuno-fluorescence during early stages of poliovirus infections to track viral receptor binding, internalization and RNA uncoating.

Another aspect of recoded viral variants that is important to explore is sensitivity to drugs that inhibit various cellular transcription factors. Recent findings show that variants of echovirus 7 that are attenuated due to increased frequencies of CpG recover

from attenuation in the presence of C16, a selective inhibitor of PKR, CDK2 and CDK5 [53]. The reason for the recovery is not entirely understood, but it shows that the specific virus is not attenuated due to morphological changes in the virion, but rather relates to host cell factors.

Studies are currently underway in the lab to understand the effects of codon pair bias in Vesicular Stomatitis Virus (VSV) and Dengue virus. Both viruses are capable of living in insect and mammalian cells, which have drastically different genetic patterns and codon pair scores. It is expected that studying the phenomenon in diverse viruses will generate general rules about the effect of codon pair deoptimization in viruses. Additionally, after characterization of these viruses in cell culture, they will be tested in appropriate animal models in hopes of unveiling appropriate vaccine candidates. Furthermore, these viruses, as well as already described polioviruses, will be the subject of ribosome profiling assays that will determine what genetic patterns are inhibiting the progression of ribosomes along a messenger.

The codon pair bias phenomenon can be extended outside of virology or bacteriology and can be used simply to alter gene expression. In particular, the present results suggest that one can increase or decrease the CpG content of a gene to alter gene expression. These strategies can be used to better express a gene from one species in the cells of another species, by following the genetic patterns of the host cell. The lab is interested in recoding a reporter gene to include different features and transfecting the gene variants in various cell types to assess differences in the activity of the reporter as a function of its environment.

Finally, competition assays are being conducted to analyze the fitness of various recoded viruses that have been synthesized. For example, polioviruses with recoded portions of P2 or P3 regions are being competed with one another to determine their relative fitness. In this manner, all of the synthetic polioviruses that have been produced in the lab thus far can be ordered from most to least attenuated. Such experiments can help determine which regions are most sensitive to recoding and what features are of the designs are most influential to attenuation.

Chapter 8: Materials and Methods

Assembly of Viral Variants

Newly designed poliovirus cDNA P1 fragments for P1-CG^{hi} and P1-CPB^{lo}UA^{hi} were synthesized de novo by Mr. Gene GmbH (Regensburg, Germany), each in two carrier plasmids. At a later time, cDNA for P1-UA^{hi} and P1-CPB^{lo} was synthesized de novo by GeneArt® (Life Technologies) each in individual carrier plasmids. In both cases, P1 fragments were removed from the carrier plasmids and inserted into a pT7-PVM plasmid in place of the wild type P1 sequence. pT7-PVM contains a full-length infectious cDNA clone of PV(M) downstream of a T7 RNA polymerase promoter. Plasmids were transformed in DH5α competent E. coli for selection and amplification, then isolated using Qiagen's Miniprep kit.

All of the synthetically generated plasmids, as well as the original WT plasmid, were linearized using a restriction enzyme containing a single site upstream of the T7 promoter. The DNA was then incubated with T7 RNA polymerase in order to transcribe positive sense RNA encoding the poliovirus polyprotein in vitro. Equal concentrations of RNA were then transfected into approximately 2x10^5 HeLa R19 cells (which were maintained as monolayers at 37°C in Dulbecco's Modified Eagle Medium (DMEM) with 10% bovine calf serum (BCS), 100 units of penicillin, and 100 mg of streptomycin per milliliter) in 35mm cell culture dishes. Specifically, RNA was incubated with a 0.5mg/ml solution of diethylaminoethyl (DEAE)-Dextran/Hank's Balanced Salt Solution (HBSS) for thirty minutes at 4°C. This mixture was then applied to cells, which had been washed

twice with HBSS. Following a thirty minute incubation with gentle rocking at room temperature, 1 ml of DMEM was added to cells and incubated for one hour at 37°C. Media was then replaced by 2% BCS in DMEM and cells were transferred to 37°C. A negative control was included in which transfection reagents were applied to cells in the absence of infectious RNA to ensure that transfection is not causing cell toxicity.

Cells were monitored for typical visual characteristics when infected with poliovirus, namely morphological changes to cell membrane, rounding of cells, and release of cells from adhesion to plate. At this point of infection, known as complete cytopathic effect (cpe), all the dishes were frozen at -80°C then thawed at room temperature three times to lyse the cells thereby releasing the viral particles into the media. Media was collected and cell debris was pelleted by low speed centrifugation. These transfection stocks were used to amplify the virus for further use.

Purification of Viral Particles

To amplify and purify virus, two 15 cm dishes of HeLa cells were washed once with HBSS, then infected with wild type or synthetic virus at a multiplicity of infection (MOI) of 1 and incubated at 37°C until cytopathic effect (CPE) was observed (2-3 days). Cells were completely lysed by three freeze/thaw cycles and cell debris was cleared by two rounds of low-speed centrifugation: 3,000 x g for 15 minutes followed by 10,000 x g for 15 minutes in a new tube. Supernatant was subjected to RNAse A digestion for 1 hour to destroy free RNA. Sodium dodecyl sulfate (SDS) and ethylenediaminetetraacetic acid (EDTA) were added to the virus to final concentrations of 0.5% and 2mM respectively, to effectively denature all cellular proteins and viral proteins that are not part of mature or intact virions [14]. Finally, virus was purified by ultracentrifugation on a 30% sucrose cushion in a swinging rotor bucket (SW28) for 4 hours at 28,000 rpm at 15°C. Media and sucrose were carefully removed and the sides and bottoms of the tubes were gently washed with HBSS to remove residue. Viral particles at the bottom of the tubes were resuspended into phosphate buffered saline (PBS) and aliquoted for storage at -80°C.

Viral Titering

Plaque assays were used to determine viral titers. Specifically, ten-fold serial dilutions of virus were used to infect cells in 6-well dishes. The cells were rocked at room temperature for 30 minutes then the virus was aspirated from the cells and replaced with a 0.6% tragacanth gum/ Minimum Essential Media (MEM) mixture containing 2% BCS. Plates were incubated at 37°C for two days then the gum mixture was removed and cells were stained with crystal violet dye. A successful viral infection within a cell will kill and lyse that cell, effectively releasing newly formed virus into the media. The gum overlay ensures that the viral particles remain localized and infect only the surrounding cells. Within 48 hours each initial infection will have resulted in a plaque in the monolayer (which is otherwise dyed from the crystal violet solution). Plaques were counted and used to determine the concentration of plaque forming units (PFU) in the virus stock.

Analysis of Viral Growth

A single-step growth experiment with wild type or synthetic viruses was conducted by infecting HeLa cells in 35mm dishes with 10 MOI of purified virus in 300 μl of media. The virus was aspirated after rocking the dishes at room temperature for 30 minutes and replaced with 2 ml 2% BCS in DMEM. The cells were moved to 37°C (0 hr) then frozen at 0, 2, 4, 7, 10 and 24 hours post infection. Following three freeze/thaw cycles and clearing of cell debris, the supernatants were subjected to plaque assays for viral titering. Two independent repetitions of the growth curve were conducted with similar trends both times. One representative curve is shown.

Determination of Viral Protein Production

To determine viral protein production, HeLa R19 cells in 24-well dishes were washed once with HBSS and infected with 10 MOI of purified virus then rocked at room temperature for thirty minutes. Virus was aspirated and replaced with DMEM with 2% BCS then plates were incubated at 37°C for 5 hours. Media was removed and cell layers were washed with PBS then lysed in 200 μl lysis buffer. 10 μl of each sample was run on a 12.5% SDS-PAGE gel then transferred to a polyvinylidene fluoride (PVDF) membrane. Membranes were blotted with anti-2C monoclonal antibodies (1:200 concentration) to evaluate $2C^{ATPase}$ proteins as an indication of the level of polyprotein translation. Bands were visualized by horseradish peroxidase chemiluminescence. The membrane was stripped and reprobed for β-actin (1:1000 concentration) in order to provide a loading control. Band intensities were calculated by ImageJ and normalized to β-actin as an internal control then expressed as a percentage of wild type (Figure 3.1).

Determination of Viral Translation Using Luciferase Proxy

The modified or wild type P1 regions of the viruses were cloned upstream of a Green *Renilla* Luciferase gene in a reporter plasmid containing a T7 RNA polymerase promoter (Thermo Scientific). Cloning was done such that translation would begin at the start site of the capsid protein and continue through the *Renilla* gene, resulting in a P1-*Renilla* luciferase fusion protein. RNA was transcribed *in vitro* from these plasmids and a separate plasmid containing only a firefly luciferase gene (FLuc) for the purpose of an internal control (Fig 3.2A). All the RNAs were then capped by a Vaccinia virus capping enzyme (New England Biolabs) [73,74]. The P1-RLuc encoding RNA for each variant was cotransfected with an FLuc encoding RNA into HeLa cells in triplicates in 24-well plates using Lipofectamine 2000 Reagent (Invitrogen) as per the manufacturer's instructions.

In this manner, the cells in each well translate a protein consisting of a synthetic or WT P1 polypeptide fused upstream of the *Renilla* luciferase protein as well as a separate firefly luciferase protein. Six hours post transfection, cells were washed with PBS and lysed in 100 μl of passive lysis buffer (Promega). Expression levels of the two luciferase proteins were assayed at 6 hours post transfection. Specifically, luciferase readings were taken using equal volumes of lysate and Promega's Dual Luciferase reagents and read with an Optocomp luminometer (GEM Biomedical). RLuc activity, a proxy for translation of P1, was normalized by FLuc activity, a control for transfection efficiency.

Analysis of Viral RNA Levels During Infection

HeLa cells in 35 mm dishes were infected with 10 MOI of virus, rocked at room temperature for 30 minutes, then media was replaced with 2 ml DMEM. Plates were moved to 37°C (0 hrs) and at 0, 4, 5, and 6 hours media was removed. Total RNA was isolated using Qiagen's RNeasy mini kit and RNA was resuspended in 30 μl RNase free water. Another set of infections was carried out in parallel in which 2mM of guanidine hydrochloride (GnHCl), a potent inhibitor of RNA replication [9] was added to the cells at 4 hours post infection. The cells were then incubated for an additional 1 or 2 hours, at which points RNA was also isolated for Northern blot analysis.

Northern blots were conducted using a negative strand digoxigenin labeled RNA probe and chemiluminescent detection with CDP-*Star* by Roche, as per manufacturer's instructions. Briefly, RNA was denatured at 68°C then run on a 1% agarose/ formaldehyde gel. The RNA from the gels was then transferred onto a nylon membrane, which was then probed for the positive strand RNA in question. The RNA probe localized to the 391 nucleotides at the 3' end of the poliovirus genome, a region which is conserved for all the viruses used.

Characterization of Type I Interferon Protein Production

Infections in HeLa cells with WT or P1-CG^{hi} were carried out with an MOI of 1 or 10 of each virus on 35 mm culture dishes, including a mock infection and transfection with 2μg Poly I:C as a positive control. Poly I:C is a dsRNA analogue known to induce an interferon response [61]. The infections were allowed to proceed for 4, 8, or 12 hours (IFNα) or 2, 4, and 6 hours (IFNβ) at which point supernatant was collected and analyzed by ELISA using an Antigenix America Inc. cytokine ELISA kit for human IFNα or β. The ELISAs were carried out according to the manufacturer's instructions in duplicate samples. The kits included ready to use 96-well plates that were precoated with IFNα or β antibodies. After incubation for one hour with supernatants, plates were washed 4 times and a biotin labeled tracer antibody was added and allowed to bind antigen for one hour. Wash steps were repeated and Streptavidin-HRP was added to the wells. After a final set of washes, tetramethylbenzidine (TMB) substrate was incubated in the wells for 15 minutes before combining with sulfuric acid to stop color development. Plates were read in a plate reader at 450 nm shortly thereafter. All washes and incubations were done at room temperature. The absorbance results were converted into protein concentrations based on standard curves that were run in parallel using proteins samples of known concentrations.

Quantification of IFNβ RNA

HeLa cell monolayers in 35mm dishes were infected in triplicates with 3 MOI of P1-WT or P1-CG^{hi}, 150 hemagglutinin units (HAU) of Newcastle Disease Virus (NDV, which served as a positive control), or mock infected and rocked at room temperature for 30 minutes (1.5 hours for NDV). The virus was then aspirated and replaced with 2 ml DMEM, 2% BCS. The plates were transferred to 37°C and at 2, 4 or 6 hours post infection (6 hours for NDV), media was removed and total RNA was extracted using Qiagen's RNeasy kit and resuspended in 30 μl volume RNase-free water. RNA samples were subjected to DNase digestion using 0.5 μl of Turbo DNase (Life Technologies) per 5 μg of RNA in 15 μl volume for 30 minutes at 37°C and then analyzed for IFNβ RNA levels by quantitative RT-PCR using Promega's SYBR Green qRT-PCR kit. The experiment was conducted on a StepOne Real Time PCR system (Applied Biosystems) using StepOne Software v2.1 for cycling and analysis. To run the qRT-PCR, an annealing temperature of 55°C was used and extension lasted 45 seconds at 72°C. Amplicon lengths were 158 nt and 218 nt for IFNβ and GAPDH, respectively, using the following primer pairs:

IFNβ	5'CATTACCTGAAGGCCAAGGA3' & 5'CAGCATCTGCTGGTTGAAGA3'
GAPDH	5'GAGTCAACGGATTTGGTCGT3' & 5'TTGATTTTGGAGGGATCTCG3'

Averages of the triplicate samples are expressed in Figure 4.3 as fold change from a mock infected plate using the $\Delta\Delta C_T$ method.

Detection of IFNβ Promoter Stimulation

A plasmid (depicted in Figure 4.4A) containing a firefly luciferase reporter gene under the control of an IFNβ promoter sequence was transfected into HeLa cells in 24-well plates (800 ng/well) in combination with another plasmid containing the *Renilla* luciferase gene (160 ng/well) to serve as an internal control. Lipofectamine 2000 Transfection Reagent (Life Technologies) was used according to the manufacturer's instructions. Following overnight transfection, the cells were infected with 10 MOI of P1-WT or P1-CG^{hi} virus, or mock infected, in triplicates. After a 30 minute incubation at room temperature, the virus was aspirated and media was replaced with DMEM with 2% BCS. Cells were incubated at 37 °C for 5 hours when supernatant was analyzed for luciferase activity. This was done in the same manner as the luciferase translation assays described in chapter 3.

Investigation of Viral Fitness by Competition Assays

The synthetic (PV-SD or PV-Max) and wild type polioviruses were used to coinfect HeLa cells using an MOI of 5 for each virus. Infections were carried out as usual and were allowed to proceed for 24 hours. Cell debris was cleared and the resulting virus pool (now a combination of PV-SD and WT or PV-Max and WT) was titered by plaque assay and was subsequently used to infect a naïve monolayer of HeLa cells with a combined MOI of 10 in the same manner. The viruses were passaged as such ten or more times. At given intervals, total RNA was harvested from the cells using Qiagen's RNeasy kit and subjected to DNase digestion using 0.5 μl of Turbo DNase (Life Technologies) per 5 μg of RNA in 15 μl volume for 30 minutes at 37°C. RNA samples were analyzed for respective viral RNA levels by quantitative RT-PCR using Promega's SYBR Green qRT-PCR kit and primers specific to each virus and primers specific for GAPDH mRNA to serve as an internal control (Table 6.1). The experiments were conducted on a StepOne Real Time PCR system (Applied Biosystems) using StepOne Software v2.1 for cycling and analysis. To run the qRT-PCR, an annealing temperature of 54°C was used and extension lasted 15 seconds at 72°C.

References

1. Kitamura N, Semler BL, Rothberg PG, Larsen GR, Adler CJ, et al. (1981) Primary structure, gene organization and polypeptide expression of poliovirus RNA. Nature 291: 547-553.
2. Mendelsohn CL, Wimmer E, Racaniello VR (1989) Cellular receptor for poliovirus: molecular cloning, nucleotide sequence, and expression of a new member of the immunoglobulin superfamily. Cell 56: 855-865.
3. Gomez Yafal A, Kaplan G, Racaniello VR, Hogle JM (1993) Characterization of poliovirus conformational alteration mediated by soluble cell receptors. Virology 197: 501-505.
4. Brandenburg B, Lee LY, Lakadamyali M, Rust MJ, Zhuang X, et al. (2007) Imaging poliovirus entry in live cells. PLoS Biol 5: e183.
5. Nomoto A, Kitamura N, Golini F, Wimmer E (1977) The 5'-terminal structures of poliovirion RNA and poliovirus mRNA differ only in the genome-linked protein VPg. Proc Natl Acad Sci U S A 74: 5345-5349.
6. Jang SK, Pestova TV, Hellen CU, Witherell GW, Wimmer E (1990) Cap-independent translation of picornavirus RNAs: structure and function of the internal ribosomal entry site. Enzyme 44: 292-309.
7. De Jesus NH (2007) Epidemics to eradication: the modern history of poliomyelitis. Virol J 4: 70.
8. Hellen CU, Facke M, Krausslich HG, Lee CK, Wimmer E (1991) Characterization of poliovirus 2A proteinase by mutational analysis: residues required for autocatalytic activity are essential for induction of cleavage of eukaryotic initiation factor 4F polypeptide p220. J Virol 65: 4226-4231.
9. Wimmer E, Hellen CU, Cao X (1993) Genetics of poliovirus. Annu Rev Genet 27: 353-436.
10. Hogle JM, Chow M, Filman DJ (1985) Three-dimensional structure of poliovirus at 2.9 A resolution. Science 229: 1358-1365.
11. Racaniello VR (1996) Early events in poliovirus infection: virus-receptor interactions. Proc Natl Acad Sci U S A 93: 11378-11381.
12. Krausslich HG, Nicklin MJ, Lee CK, Wimmer E (1988) Polyprotein processing in picornavirus replication. Biochimie 70: 119-130.
13. B. N. Fields DMK RMC, J.L. Melnick, B. Roizman (1985) Picornaviruses and their replication; RE S, editor. New York, NY: Raven Press.
14. Mueller S, Wimmer E, Cello J (2005) Poliovirus and poliomyelitis: a tale of guts, brains, and an accidental event. Virus Res 111: 175-193.
15. Salk JE, Krech U, Youngner JS, Bennett BL, Lewis LJ, et al. (1954) Formaldehyde treatment and safety testing of experimental poliomyelitis vaccines. Am J Public Health Nations Health 44: 563-570.
16. Sabin AB (1957) Properties and behavior of orally administered attenuated poliovirus vaccine. J Am Med Assoc 164: 1216-1223.
17. WHO (2010) Global Polio Eradication Initiative. http://www.polioeradication.org/ Accessed May 1, 2014.
18. Koch G (1973) Interaction of poliovirus-specific RNAs with HeLa cells and E. coli. Curr Top Microbiol Immunol 62: 89-138.
19. Flanegan JB, Petterson RF, Ambros V, Hewlett NJ, Baltimore D (1977) Covalent linkage of a protein to a defined nucleotide sequence at the 5'-terminus of virion and replicative intermediate RNAs of poliovirus. Proc Natl Acad Sci U S A 74: 961-965.
20. Racaniello VR, Baltimore D (1981) Cloned poliovirus complementary DNA is infectious in mammalian cells. Science 214: 916-919.

21. Semler BL, Dorner AJ, Wimmer E (1984) Production of infectious poliovirus from cloned cDNA is dramatically increased by SV40 transcription and replication signals. Nucleic Acids Res 12: 5123-5141.
22. van der Werf S, Bradley J, Wimmer E, Studier FW, Dunn JJ (1986) Synthesis of infectious poliovirus RNA by purified T7 RNA polymerase. Proc Natl Acad Sci U S A 83: 2330-2334.
23. Molla A, Paul AV, Wimmer E (1991) Cell-free, de novo synthesis of poliovirus. Science 254: 1647-1651.
24. Cello J, Paul AV, Wimmer E (2002) Chemical synthesis of poliovirus cDNA: generation of infectious virus in the absence of natural template. Science 297: 1016-1018.
25. Song Y, Liu Y, Ward CB, Mueller S, Futcher B, et al. (2012) Identification of two functionally redundant RNA elements in the coding sequence of poliovirus using computer-generated design. Proc Natl Acad Sci U S A 109: 14301-14307.
26. Gustafsson C, Govindarajan S, Minshull J (2004) Codon bias and heterologous protein expression. Trends Biotechnol 22: 346-353.
27. Mueller S, Papamichail D, Coleman JR, Skiena S, Wimmer E (2006) Reduction of the rate of poliovirus protein synthesis through large-scale codon deoptimization causes attenuation of viral virulence by lowering specific infectivity. J Virol 80: 9687-9696.
28. Barclay W, Li Q, Hutchinson G, Moon D, Richardson A, et al. (1998) Encapsidation studies of poliovirus subgenomic replicons. J Gen Virol 79 (Pt 7): 1725-1734.
29. Coleman JR, Papamichail D, Skiena S, Futcher B, Wimmer E, et al. (2008) Virus attenuation by genome-scale changes in codon pair bias. Science 320: 1784-1787.
30. Ren RB, Costantini F, Gorgacz EJ, Lee JJ, Racaniello VR (1990) Transgenic mice expressing a human poliovirus receptor: a new model for poliomyelitis. Cell 63: 353-362.
31. Koike S, Taya C, Kurata T, Abe S, Ise I, et al. (1991) Transgenic mice susceptible to poliovirus. Proc Natl Acad Sci U S A 88: 951-955.
32. Mueller S, Coleman JR, Papamichail D, Ward CB, Nimnual A, et al. (2010) Live attenuated influenza virus vaccines by computer-aided rational design. Nat Biotechnol 28: 723-726.
33. Yang C, Skiena S, Futcher B, Mueller S, Wimmer E (2013) Deliberate reduction of hemagglutinin and neuraminidase expression of influenza virus leads to an ultraprotective live vaccine in mice. Proc Natl Acad Sci U S A 110: 9481-9486.
34. Coleman JR, Papamichail D, Yano M, Garcia-Suarez Mdel M, Pirofski LA (2011) Designed reduction of Streptococcus pneumoniae pathogenicity via synthetic changes in virulence factor codon-pair bias. J Infect Dis 203: 1264-1273.
35. Josse J, Kaiser AD, Kornberg A (1961) Enzymatic synthesis of deoxyribonucleic acid. VIII. Frequencies of nearest neighbor base sequences in deoxyribonucleic acid. J Biol Chem 236: 864-875.
36. Swartz MN, Trautner TA, Kornberg A (1962) Enzymatic synthesis of deoxyribonucleic acid. XI. Further studies on nearest neighbor base sequences in deoxyribonucleic acids. J Biol Chem 237: 1961-1967.
37. Nussinov R (1981) Nearest neighbor nucleotide patterns. Structural and biological implications. J Biol Chem 256: 8458-8462.
38. Nussinov R (1984) Doublet frequencies in evolutionary distinct groups. Nucleic Acids Res 12: 1749-1763.
39. Rima BK, McFerran NV (1997) Dinucleotide and stop codon frequencies in single-stranded RNA viruses. J Gen Virol 78 (Pt 11): 2859-2870.
40. Rothberg PG, Wimmer E (1981) Mononucleotide and dinucleotide frequencies, and codon usage in poliovirion RNA. Nucleic Acids Res 9: 6221-6229.

41. Beutler E, Gelbart T, Han JH, Koziol JA, Beutler B (1989) Evolution of the genome and the genetic code: selection at the dinucleotide level by methylation and polyribonucleotide cleavage. Proc Natl Acad Sci U S A 86: 192-196.
42. Qiu L, Moreira A, Kaplan G, Levitz R, Wang JY, et al. (1998) Degradation of hammerhead ribozymes by human ribonucleases. Mol Gen Genet 258: 352-362.
43. Duan J, Antezana MA (2003) Mammalian mutation pressure, synonymous codon choice, and mRNA degradation. J Mol Evol 57: 694-701.
44. Ehrlich M, Wang RY (1981) 5-Methylcytosine in eukaryotic DNA. Science 212: 1350-1357.
45. Coulondre C, Miller JH, Farabaugh PJ, Gilbert W (1978) Molecular basis of base substitution hotspots in Escherichia coli. Nature 274: 775-780.
46. Bird AP (1980) DNA methylation and the frequency of CpG in animal DNA. Nucleic Acids Res 8: 1499-1504.
47. Krieg AM, Yi AK, Matson S, Waldschmidt TJ, Bishop GA, et al. (1995) CpG motifs in bacterial DNA trigger direct B-cell activation. Nature 374: 546-549.
48. Klinman DM, Yi AK, Beaucage SL, Conover J, Krieg AM (1996) CpG motifs present in bacteria DNA rapidly induce lymphocytes to secrete interleukin 6, interleukin 12, and interferon gamma. Proc Natl Acad Sci U S A 93: 2879-2883.
49. Yi AK, Klinman DM, Martin TL, Matson S, Krieg AM (1996) Rapid immune activation by CpG motifs in bacterial DNA. Systemic induction of IL-6 transcription through an antioxidant-sensitive pathway. J Immunol 157: 5394-5402.
50. Sugiyama T, Gursel M, Takeshita F, Coban C, Conover J, et al. (2005) CpG RNA: identification of novel single-stranded RNA that stimulates human CD14+CD11c+ monocytes. J Immunol 174: 2273-2279.
51. Burns CC, Campagnoli R, Shaw J, Vincent A, Jorba J, et al. (2009) Genetic inactivation of poliovirus infectivity by increasing the frequencies of CpG and UpA dinucleotides within and across synonymous capsid region codons. J Virol 83: 9957-9969.
52. Burns CC, Shaw J, Campagnoli R, Jorba J, Vincent A, et al. (2006) Modulation of poliovirus replicative fitness in HeLa cells by deoptimization of synonymous codon usage in the capsid region. J Virol 80: 3259-3272.
53. Atkinson NJ, Witteveldt J, Evans DJ, Simmonds P (2014) The influence of CpG and UpA dinucleotide frequencies on RNA virus replication and characterization of the innate cellular pathways underlying virus attenuation and enhanced replication. Nucleic Acids Res 42: 4527-4545.
54. (2006) Exploring the Role of Antiviral Drugs in the Eradication of Polio: Workshop Report: The National Academies Press.
55. Joklik WK, Darnell JE, Jr. (1961) The adsorption and early fate of purified poliovirus in HeLa cells. Virology 13: 439-447.
56. Schwerdt CE, Fogh J (1957) The ratio of physical particles per infectious unit observed for poliomyelitis viruses. Virology 4: 41-52.
57. Molla A, Jang SK, Paul AV, Reuer Q, Wimmer E (1992) Cardioviral internal ribosomal entry site is functional in a genetically engineered dicistronic poliovirus. Nature 356: 255-257.
58. Jacobs E, Mills JD, Janitz M (2012) The role of RNA structure in posttranscriptional regulation of gene expression. J Genet Genomics 39: 535-543.
59. Zama M (1997) Translational pauses during the synthesis of proteins and mRNA structure. Nucleic Acids Symp Ser: 179-180.
60. Kubota H (2009) Quality control against misfolded proteins in the cytosol: a network for cell survival. J Biochem 146: 609-616.

61. Fortier ME, Kent S, Ashdown H, Poole S, Boksa P, et al. (2004) The viral mimic, polyinosinic:polycytidylic acid, induces fever in rats via an interleukin-1-dependent mechanism. Am J Physiol Regul Integr Comp Physiol 287: R759-766.
62. Barral PM, Morrison JM, Drahos J, Gupta P, Sarkar D, et al. (2007) MDA-5 is cleaved in poliovirus-infected cells. J Virol 81: 3677-3684.
63. Barral PM, Sarkar D, Fisher PB, Racaniello VR (2009) RIG-I is cleaved during picornavirus infection. Virology 391: 171-176.
64. Kato H, Takeuchi O, Sato S, Yoneyama M, Yamamoto M, et al. (2006) Differential roles of MDA5 and RIG-I helicases in the recognition of RNA viruses. Nature 441: 101-105.
65. Karlin S, Doerfler W, Cardon LR (1994) Why is CpG suppressed in the genomes of virtually all small eukaryotic viruses but not in those of large eukaryotic viruses? J Virol 68: 2889-2897.
66. Herrera GA, Iwane MK, Cortese M, Brown C, Gershman K, et al. (2007) Influenza vaccine effectiveness among 50-64-year-old persons during a season of poor antigenic match between vaccine and circulating influenza virus strains: Colorado, United States, 2003-2004. Vaccine 25: 154-160.
67. Govaert TM, Thijs CT, Masurel N, Sprenger MJ, Dinant GJ, et al. (1994) The efficacy of influenza vaccination in elderly individuals. A randomized double-blind placebo-controlled trial. JAMA 272: 1661-1665.
68. Jefferson T, Rivetti A, Harnden A, Di Pietrantonj C, Demicheli V (2008) Vaccines for preventing influenza in healthy children. Cochrane Database Syst Rev: CD004879.
69. Ritzwoller DP, Bridges CB, Shetterly S, Yamasaki K, Kolczak M, et al. (2005) Effectiveness of the 2003-2004 influenza vaccine among children 6 months to 8 years of age, with 1 vs 2 doses. Pediatrics 116: 153-159.
70. Bridges CB, Thompson WW, Meltzer MI, Reeve GR, Talamonti WJ, et al. (2000) Effectiveness and cost-benefit of influenza vaccination of healthy working adults: A randomized controlled trial. JAMA 284: 1655-1663.
71. Reed LJ, Muench, M. (1938) A simple method for estimating fifty percent endpoints. Am J Hyg 27: 493-497.
72. Costafreda MI, Perez-Rodriguez FJ, D'Andrea L, Guix S, Ribes E, et al. (2014) Hepatitis a virus adaptation to cellular shutoff is driven by dynamic adjustments of codon usage and results in the selection of populations with altered capsids. J Virol 88: 5029-5041.
73. Guo PX, Moss B (1990) Interaction and mutual stabilization of the two subunits of vaccinia virus mRNA capping enzyme coexpressed in Escherichia coli. Proc Natl Acad Sci U S A 87: 4023-4027.
74. Mao X, Shuman S (1994) Intrinsic RNA (guanine-7) methyltransferase activity of the vaccinia virus capping enzyme D1 subunit is stimulated by the D12 subunit. Identification of amino acid residues in the D1 protein required for subunit association and methyl group transfer. J Biol Chem 269: 24472-24479.